BACHELOR THESIS ASSIGNMENT CIVIL ENGINEERING

EFFECT OF DESICCATION CRACKING ON DIKE FAILURE DUE TO BACKWARD EROSION PIPING

ARNOLD HEMPEL

APRIL - JULY 2024

UNIVERSITY OF TWENTE.

Image by Hilda Weges, 2018

EFFECT OF DESICCATION CRACKING ON DIKE FAILURE DUE TO BACKWARD EROSION PIPING

Student:

Name:	Arnold Hempel
Student Number:	S2627434
E-mail address:	a.hempelliziano@student.utwente.nl

Internal supervisor:

Name:	dr. Hongyang Cheng
E-mail address:	h.cheng@utwente.nl

Educational program:

Institute:	University of Twente
Faculty:	Engineering Technology
Department:	Civil Engineering and Management

Period: April 2024 - July 2024

PREFACE

This thesis completes the three-year bachelor of Civil Engineering at the University of Twente. The assignment was done internally at the mentioned institution.

This thesis has been an invaluable experience, allowing me to push the boundaries of my knowledge and explore phenomena I was unfamiliar with. This research journey has been very rewarding, and I am thrilled for its completion. Through this undertaking, I have developed new interests in several aspects of civil engineering which I hope to further purse during my master.

I would like to thank my supervisor, dr. Hongyang Cheng for his support during the entire process. I am also grateful to my family and friends for their encouragement, especially my parents for all their support and trust.

Arnold Hempel
June, 2024

TABLE OF CONTENTS

SUMMARY

This thesis explores the effects of desiccation cracking on the failure of dikes due to backward erosion piping (BEP). As climate change continues to impact weather patterns, increasing the frequency and extreme events, such as prolonged droughts and heavy precipitations, increased formation of desiccation cracks is more likely to happen, followed by high water levels. These cracks have been linked to the degradation of soil properties, notably its hydraulic conductivity, which affects the safety of geotechnical structures. The research aims to quantify the extent to which these cracks contribute to dike failure specifically concerning BEP.

The study employs a numerical model based on a base model of a dike's cross-section, which is then modified to incorporate the characteristics of desiccation cracks, such as their number, spacing, and aperture. Through a series of numerical simulations, this thesis evaluates how these variables influence the critical hydraulic head required for pipe initiation and propagation. Results indicate that while the crack aperture and the hydraulic conductivity of the cracked layer do not significantly impact BEP, the spacing and number of cracks tend to lower the critical head necessary for pipe initiation, thereby increasing the probability of dike failure. The findings suggest that desiccation cracking primarily affects the initiation phase of BEP, creating preferential pathways for water flow and reducing the need for high hydraulic heads to achieve uplift conditions. Additionally, higher spacing and number of cracks lead to a higher variability of the critical head ranges.

In conclusion, the research emphasises the importance of considering desiccation cracking in dike safety assessments, especially in the context of climate change. Recommendations for future studies include a more detailed analysis of crack formation conditions, the effects of varying crack depths, the study of different soil types, and the interaction of desiccation cracks with other failure mechanisms to provide a more complete analysis of the effects of these fissures on overall dike stability. Such investigations could provide a more comprehensive understanding of dike vulnerabilities and aid in developing strategies for enhancing the resilience of flood protection structures.

1. INTRODUCTION

1.1 CONTEXT

Civilizations around the world have been settling near rivers for centuries. According to Gökçekuş and Bolouri (2023), around 40% of the world's population lives in transboundary river and lake basins. This has brought forth countless benefits as well as different kinds of dangers. For instance, a study projected that by 2050 a quarter of the global GDP will be produced in the 10 most populated river basins (Frontier Economics, 2012). However, river flood risk is projected to affect 134 million people by that same year (Ward & Winsemius, n.d.). The Netherlands, located at the delta of various important European rivers, has been heavily influenced by water management. Through time the small nation has become renowned for its intricate system of dikes and water management infrastructure. Nevertheless, failure of these structures is exacerbated by climate change as stated by Illés and Nagy (2022).

As global temperature continues to rise and precipitation patterns become more erratic, the frequency and severity of extreme weather events are increasing. A recent study found Europe will become dryer during the future summers (Řehoř et al., 2023). In addition, according to the four scenarios presented by KNMI'23 in the Netherlands, potential maximum precipitation deficit (once per every 10 years) is bound to increase by 2050. Furthermore, potential evaporation in all four scenarios is projected to increase by at least 6% by 2050 (KNMI'23 klimaat scenarios, 2023).

Given these projections, one aspect that is of concern is soil moisture levels. Soil moisture being highly related to evapotranspiration and precipitation is likely to decrease. Řehoř et al. (2023) suggested over the past 41 years soil moisture tended to decrease and drought frequencies increased. This trend may lead to several different effects including the rise in the creation of desiccation cracks in soil layers close to the surface.

1.2 PROBLEM STATEMENT

Desiccation cracks that occur due to low soil moisture have been linked to an increase in the failure of geotechnical structures (Foster et al., 2000, Parker and Jenne, 1967, Bernatek-Jakiel and Poesen, 2018). These fissures can lead to alterations of the soil's properties and facilitate the initiation of backward erosion piping (BEP), which is considered one of the most important failure mechanisms regarding dike safety (Robbins and van Beek, 2015).

The appearance of fissures exacerbates BEP since they provide an exit point for the seepage flow coming from the river side of the dike. If the flow is strong enough, sand will be eroded towards the hinterland, generating after some time a pipe between the impermeable layer and the aquifer. If the hydraulic head is large enough, the pipe will continue to grow towards the riverside, known as the primary erosion of BEP, eventually creating a channel connecting both sides of the dike. As erosion continues the pipe will widen (secondary erosion) leading to the collapse of the structure.

The development of desiccation cracks on Dutch clay dikes has already been reported. Van den Akker *et al.* (2013) observed clay dikes with cracks of over 1m after running field observations in the Netherlands. More recently Bottema *et al.* (2019) also mentioned the occurrence of cracks in numerous primary levees, such as the 'Oostvaardersdijk' near Lelystad which showed large fissures after the summer of 2018 which was characterized by an extreme precipitation deficit, abundant sunshine, and high temperatures. Some of these cracks can be seen in Figure 1.

Figure 1. Cracks on 'Oostvaardersdijk'. Left: 1 month after drought. Right: 9 months after drought (Bottema et al., 2019)

The vulnerability of flood defences is especially important in the Netherlands given that 60% of the country is prone to flooding (Fundamentals of Flood Protection, 2017). Currently, around 62% of primary flood defences do not comply with safety standards and 26% of these require urgent improvements (Landelijk Beeld van de Staat van de Primaire Waterkeringen, 2023). Figure 2 shows how river dikes have the lowest safety category among all the dikes in the country and at the same time their failure would lead to the highest water depths. River dike failure is in turn an important problem in the Netherlands.

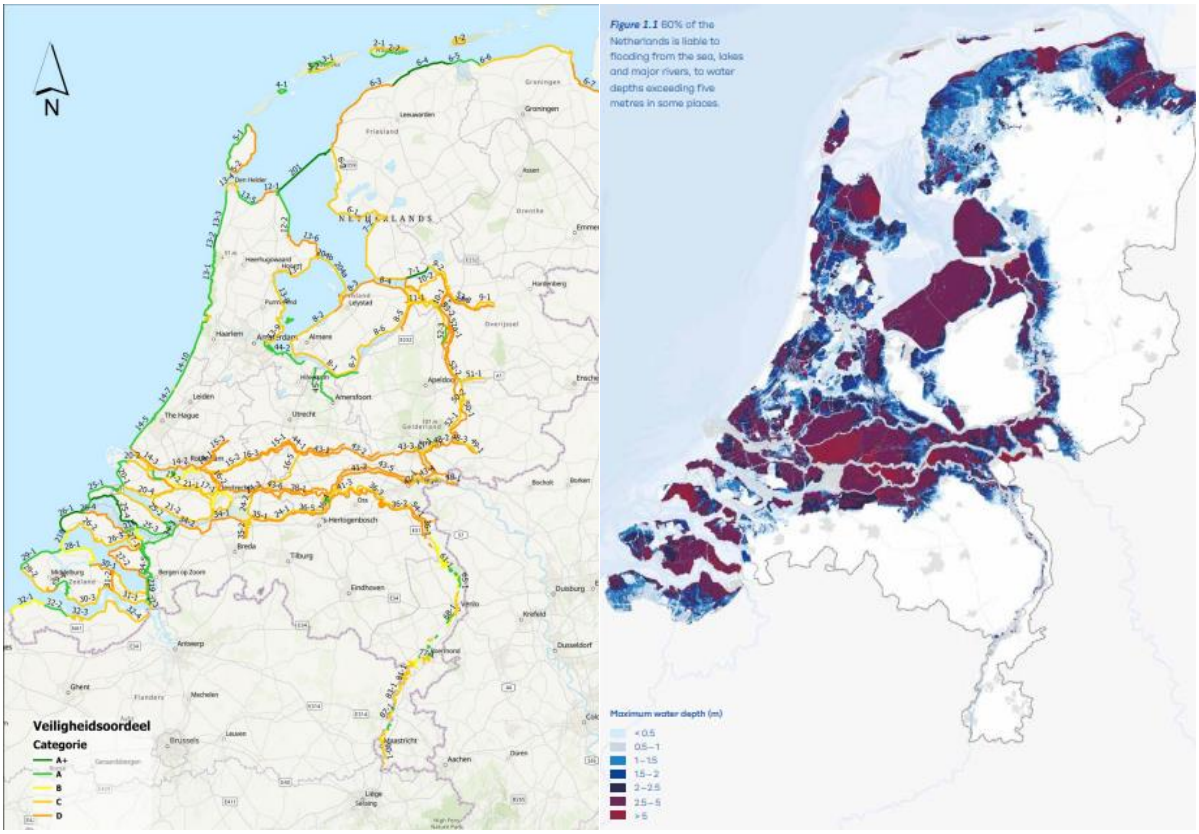

Figure 2. Right: Safety category of Dutch dikes (Landelijk Beeld van de Staat van de Primaire Waterkeringen, 2023), Left: Maximum water levels (Fundamentals of Flood Protection, 2017)

1.3 RESEARCH RELEVANCE

In 2017, the approach towards flood protection in the Netherlands changed to consider more than just water levels. The new safety standards place more focus on the failure mechanisms (Fundamentals of Flood Protection, 2017). In addition, given the impact that climate change is expected to have, more research is being conducted regarding models for BEP (van Beek, 2015). However, there still is a gap in knowledge regarding the degree to which desiccation cracks affect dike safety considering piping.

The recent observations of desiccation cracks in Dutch dikes and the linked increase in failure of geotechnical structures due to these fissures make their study highly relevant to provide valuable insight into Dutch dike vulnerabilities related to the evolving climate change threat. Understanding the factors driving dike failure, particularly desiccation cracks leading to piping is crucial to maintain the climate resilience of the flood defences for current and future conditions.

1.4 RESEARCH OBJECTIVE

The main objective of this thesis is to analyse through a numerical model the impact of severe drought on the probability of failure of Dutch dikes, specifically through the study of the effect of desiccation cracking in the blanket layer on the critical head at which backward erosion leads to dike failure. BEP was specifically chosen since as previously mentioned it is one of the main failure mechanisms and the link with severe droughts has not been previously studied in depth.

1.5 RESEARCH QUESTIONS

Regarding the main objective of the thesis, the following main question is formulated:

To what degree does desiccation cracking influence dike failure due to backwards erosion piping?

To delimit the broad aim, set by the main question and provide a more structured approach to the investigation several sub-questions have been created.

1. Which characteristics of desiccation cracks should be considered when studying their effect on BEP and to what extent do they influence the propagation of pipes?
2. How can the complexity of desiccation cracks be implemented into a model regarding BEP?
3. To what extent is BEP influenced by the degree of cracking of the blanket layer?

1.6 RESEARCH APPROACH

According to Verschuren and Doorewaard (2010), a research strategy is a set of key decisions, starting by choosing either broadness or depth. This thesis will focus on a broad view of desiccation cracking effects on BEP in dikes. An in-depth study will not be pursued due to the limited amount of time and resources available. Nevertheless, a general view is considered sufficient to better understand the possible dangers brought on by this phenomenon and find possible correlations between studied variables.

Furthermore, the strategy is to focus on both quantification and qualification to answer the proposed research questions. While some of the questions are better addressed with quantifiable data others such

as sub-question 2 require a qualitative response. In turn, a combination of both types of answers will provide a more complete understanding of desiccation cracking effects on BEP.

Moreover, the study will not be empirical. The strategy is to focus on a theoretical approach due to limited resources to carry out the thesis. To produce an empirical study a large-scale experiment on a constructed dike would have to be undertaken. Due to the large amounts of financial and temporal resources needed for this, it was decided to better focus on the theoretical aspects rather than real-world experimentation.

Since the strategy is to focus on a theoretical, quantitative, and in-depth study to achieve the proposed objective, the selected research methods are literature review and computational simulation. These methods are highly advantageous since research can easily be conducted to study changes in a predefined situation. Additionally, they can be done within a limited time and without the need for large amounts of resources. According to Verschuren and Doorewaard (2010), these methods ensure a high degree of internal validity since no external variables affect the results as in an empirical study. Nevertheless, representability of the real world is a disadvantage since it will never be an exact match of the real situation.

1.7 THESIS OUTLINE

This section will explain in general the thesis' structure to answer the proposed questions. Section 2 will provide background information regarding flood defences, piping, and desiccation cracks. Furthermore, Section 3 will address important concepts, phenomena, and rules which will be used throughout the thesis. Sections 3.3 and 3.4 will specifically dwell on desiccation cracking effects on soil properties and geometrical features and in turn address part of the first two sub-questions through an in-depth literature review. Subsequently, sections 4.2 and 4.3 will address the base model and its setup, which will be used primarily for verification purposes. Section 4.4 will address the modifications made to the base model to incorporate the cracks in the hinterland and develop the cracked model. This section will finish answering the second sub-question. The following section will then explain the format that will be implemented to study the proposed cases or numerical simulations. The results of said simulations will then be presented and discussed to provide answers to sub-questions 1 and 3. Sections 7 and 8 will cover the conclusions and provide recommendations for further research.

2. BACKGROUND

2.1 FLOOD DEFENCES

Flood defences are structures designed to protect an area from flooding along the coast, rivers, and other bodies of water (Jonkman, 2014). Due to the position of the Netherlands in the deltas of several large rivers and its low-lying nature, around 60% of the country is vulnerable to floods. In turn, the flood defences have been a critical part of the nation for hundreds of years. Nevertheless, it was after the 1953 storm surge where 1836 people died that the approach to flood protection changed. Statistical analysis was central in this approach considering safety standards were based on the probability of exceeding a specific water level (Fundamentals of Flood Protection, 2017).

In 2017, the approach was further modified, by basing standards on risk probability. Risk not only included the probability of flooding but also the consequences of a flood. Flood probability is defined

as the probability of the loss of flood defence capacity in a levee segment causing the area protected by the levee segment to flood in a way that fatalities or substantial economic damage occur (Fundamentals of Flood Protection, 2017). By considering the probability of flooding, geotechnical failure mechanisms started to be considered as in the exceedance probability approach they were not. This led to many dikes not complying with the set safety standards. In turn, considering the different failure mechanisms which affect the flood defences has become highly important and will be further discussed below.

2.1.1 Dikes

Flood defences can be categorized into several types including dikes or levees, dams, dunes and many more. Dikes are earthen structures with sufficient elevation and strength to be able to retain water under extreme circumstances (Jonkman, 2014). They can either be coastal dikes which protect against flooding from the sea or river dikes which as the name suggests, protect against floods from the rivers. The latter is the focus of this thesis and an example can be seen in Figure 3.

These structures commonly have a trapezoidal form and consist of several different types of soils including sand, peat and clay. Their dimensions will be determined by the loads they are exposed to. Newer dikes consist of a sand core and a blanket layer of clay (Jonkman, 2014). River dikes are generally constructed on a sandy aquifer. The flood protection capacity of the structure is determined by its height, its shape in profile and the ground on which it stands (Fundamentals of Flood Protection, 2017).

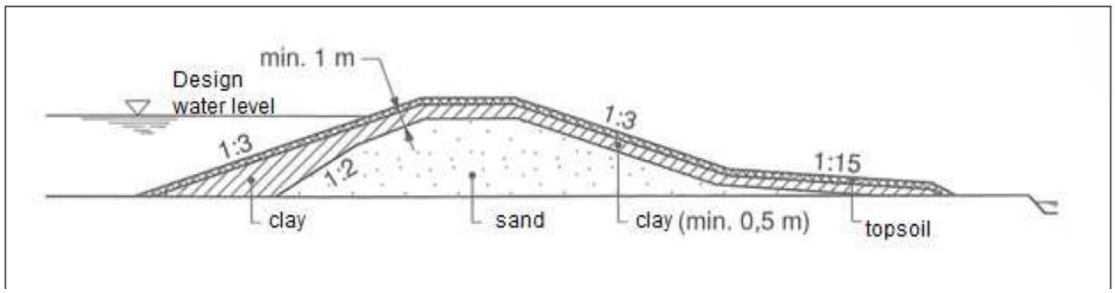

Figure 3. Typical river dike cross-section (Jonkman, 2014)

2.1.2 Failure Mechanisms

Dikes can lose their flood-protecting capabilities due to several causes usually referred to as failure mechanisms. The several different types of failure mechanisms can be seen in Figure 4. As mentioned before the different geotechnical failure mechanisms have become highly relevant since they were not specifically included in Dutch dike safety standards until 2017. While dikes are exposed to a variety of different failure mechanisms, in the Netherlands piping is one of the most dominant ones (van Esch, 2014) and will be further discussed below.

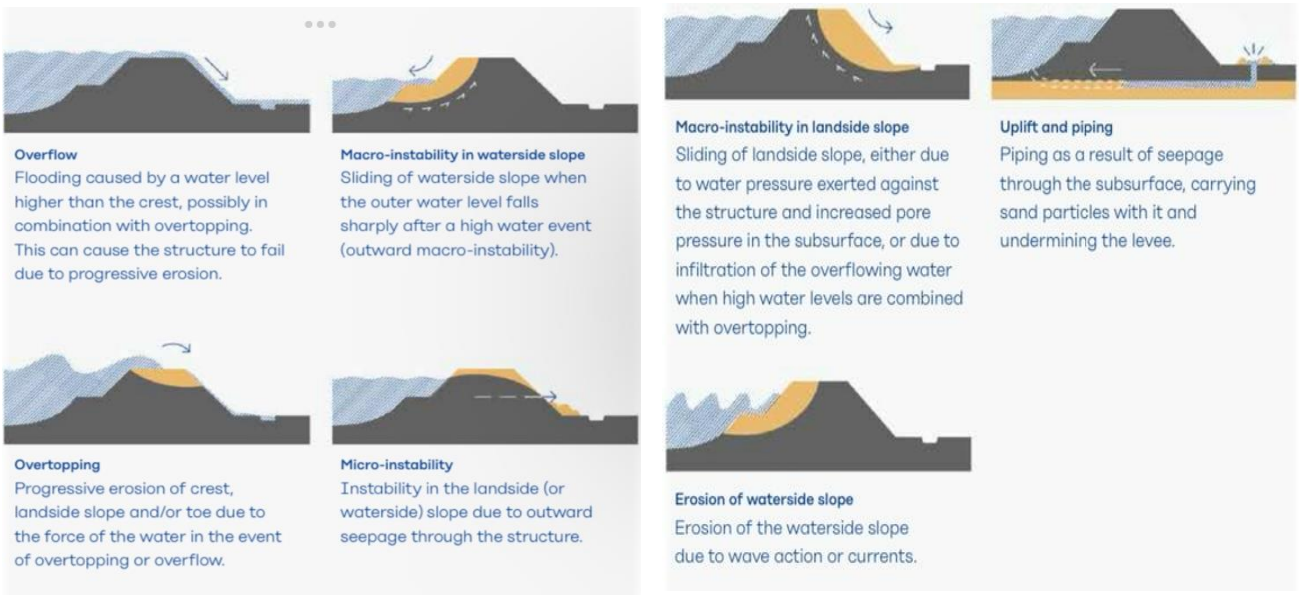

Figure 4. Dike failure mechanisms (Fundamentals of Flood Protection, 2017)

2.2 PIPING

Soil piping is a phenomenon present around the world. It occurs in several different types of climates, and topographies and in both natural and anthropogenic elements. In earth sciences, it most often refers to the formation of linear voids (pipes) by concentrated flowing water in soils or unconsolidated or poorly consolidated sediments (Bernatek-Jakiel and Poesen, 2018). It is highly difficult to detect and control since it is not a process which occurs at the surface. Piping is affected by several factors including climate, vegetation, land use, and soil type. This phenomenon covers several different processes including backward erosion piping, which is the most important one when referring to dikes in the Netherlands.

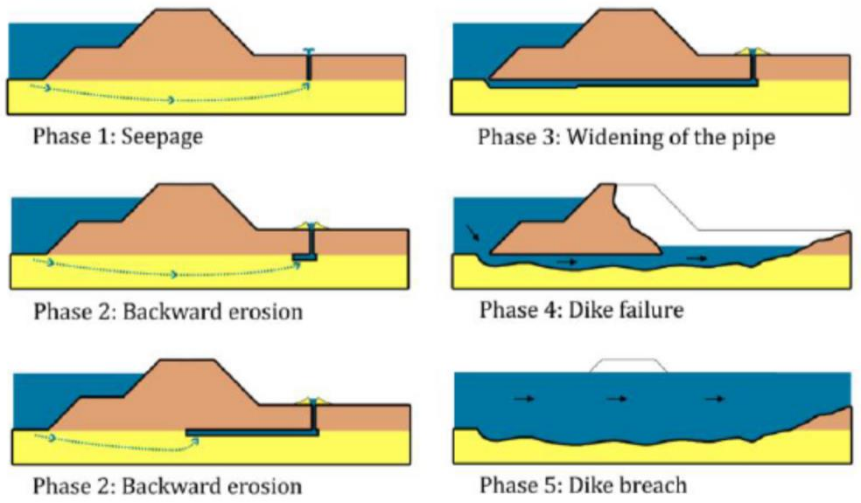

Figure 5. Phases of backwards erosion piping (Robbins and van Beek, 2015)

BEP accounts for one-third of all piping failure in dams and levees in turn making it a highly important phenomenon regarding safety (Robbins and van Beek, 2015). This phenomenon can be divided into several different phases as seen in Figure 5. While several authors discuss different phases this thesis will follow the division made by Robbins and van Beek (2015) and van Beek et al. (2013).

Before the initiation of BEP, several conditions must be met. According to Robbins and van Beek (2015), the process requires the presence of seepage in the foundation. Another condition which must be met is the existence of an open and unfiltered exit. If the water pressure generated by seepage under the blanket layer is higher than the weight of the layer, then uplift will lead to local cracking of the blanket layer creating the necessary exit (van Esch, 2014). Nevertheless, the unfiltered exit can be due to a pre-existing defect in the blanket layer or occur naturally due to the lack of a blanket layer (van Beek et al., 2013).

Once seepage and the open exit conditions are met, the initiation and progression phase of BEP is possible. Firstly, the seepage flow lines will concentrate on the exit point due to the gradient in this section being higher than that under the dike due to the lower permeability of the levee material compared to sand (van Beek et al., 2013). This concentrated flow will lead to sand boils without the presence of sand. The transport and deposition of sand will be dependent on the fluidization of sand near the exit (van Esch, 2014). Sufficient increases in the hydraulic head will lead to higher seepage velocities at the exit causing fluidization of sand from the bed which will be lifted through the exit channel and eventually deposited on the hinterland (Robbins and van Beek, 2015). The continued deposition of sand will lead to the initiation of pipes between the cohesive and sand layers.

For the pipe to be able to continue extending toward the riverside, sufficient horizontal hydraulic gradients must exist to keep sand being transported from the pipe's edge to the exit (Robbins and van Beek, 2015). It is important to note that if the flow is not enough the pipe might reach an equilibrium and sand deposition will stop. This can only be overcome with a sufficiently high head known as the critical head which will then allow for the pipe formation to progress (a process also called primary erosion) and eventually connect the upstream and downstream sides. It is important to note progression and initiation are governed by distinct mechanisms (van Beek et al., 2013). The initiation and progression phase can be seen as phase 2 in Figure 5.

The subsequent phase is called widening or secondary erosion and can be seen as phase 3 in Figure 5. This phase starts once the pipe has connected the land and river sides. With the connection of both sides, the material transport increases due to the lack of sand resistance in the channel (van Beek and Bezuijen, 2013). The pipe will then start to progressively widen from the upstream to the downstream which will allow for a larger flow leading to more widening.

The final phase mentioned by van Beek et al. (2013) is failure. With continued widening the levee can either lose stability and slide or the flow under the main body leads to deformations and eventually the dike settles after which the BEP process starts again and after various cycles, the dike collapses. Failure can be seen in the last two phases of Figure 5.

2.3 DESICCATION CRACKS

Since this thesis focuses on fissures in the clay blanket layer of Dutch dikes the effects of this phenomenon will only be discussed for clayey soils. Soil layers near or on the surface are vulnerable to cracking in the cases of long dry spells. Desiccation cracks in particular result from the loss of moisture content due to evaporation from the surface of the material. The loss of pore water will increase soil

suction, causing it to shrink (Tang et al, 2021). If soil is constrained while shrinking, horizontal tensile forces will be generated. In the case that the tensile stress surpasses the tensile strength of the material, cracks will appear (Tang et al, 2021). The formation and propagation of desiccation cracks is a highly complex phenomenon.

Adding to the complexity is the fact that clays present a swell-shrinkage behaviour. In dry conditions, clay will tend to shrink which as mentioned may cause cracks. When the soil moisture increases then clay tends to swell. It has been reported self-healing of desiccation cracks may occur upon swelling (Rayhani et al., 2007, Tian et al. 2023). Nevertheless, other studies suggest clay does not fully recover after swelling and when the soil experiences low moisture levels again cracks would probably form in the same sections, meaning the effects of cracking are permanent (Albrecht and Benson, 2001). In addition, when water is absorbed after cracking, shear strength is reduced which leads to more cracks once the soil is dry again (Rayhani et al., 2007). In turn, cracks may continue to deepen because of these shrink-swell cycles. As a result, desiccation cracks are difficult to predict and model.

3. LITERATURE REVIEW

This section explores key research and theories related to BEP and desiccation cracking, providing a summarized overview of current knowledge. The information contained in the literature review will establish a foundation for the entire thesis.

3.1 EMPIRICAL RULE OF SELLMEIJER

Various assessments have been developed through the years to determine the occurrence of piping and predict how likely a dike is to fail. Currently, safety assessments are mostly based on the rule proposed by Sellmeijer (1988), which was later revised and calibrated to the adapted Sellmeijer rule (2011). The rule works by assessing average gradients between the seepage entry and the exit point, which is combined with a seepage length to obtain a critical head difference (Teixeira et al., 2016). If this critical head is reached erosion will accelerate and eventually, a pipe connecting both sides is formed leading to failure. However, if the critical head is not surpassed a stable pipe length is achieved until the head increases. In turn, the critical head is a good parameter to analyse when studying the probability of failure of a dike due to BEP. The lower the value for the critical head, the more probable it would be for the dike to fail.

Sellmeijer et al. (2011) defined the following formula for the critical head:

$$H_c = F_{resistance} \cdot F_{scale} \cdot F_{geometry} \cdot L$$

Where:

$$F_{resistance} = \eta \cdot \tan\Theta \cdot \frac{\gamma_p}{\gamma_w}$$

$$F_{scale} = \left(\frac{d_{70,m}}{\sqrt[3]{\kappa L}}\right) \cdot \left(\frac{d_{70}}{d_{70,m}}\right)^{0.4} \text{ and } \kappa = \frac{v_w}{g} \cdot k$$

$$F_{geometry} = 0.91 \cdot \left(\frac{D}{L}\right)^{\frac{0.28}{\left(\frac{D}{L}\right)^{2.8}-1}+0.04}$$

Where:
γ_p – unit weight of submerged particles (N/m^3)
γ_w – unit weight of water (N/m^3)
η - White's constant (-)
θ - bedding angle (deg)
κ - intrinsic permeability (m^2)
L - base length (m)
d_{70} – 70 percentile value of grain size distribution (m)
$d_{70,\,m}$ – mean value of d_{70} in small scale experiments (m)
g - gravitational acceleration (m/s^2)
ν_w – kinematic viscosity of water (m^2/s)
k – hydraulic conductivity (m/s)
D – aquifer height (m)

Some of these values are constants or standard values which can be seen in Table 1.

Table 1. Standard values for revised Sellmeijer rule (Rijkswaterstaat,

Parameters	Value
Unit weight of water (kN/m^3)	10
Kinematic viscosity of water (m^2/s)	$1.33 \cdot 10^{-6}$
White's constant (-)	0.25
Bedding angle (deg)	37
Mean value of d_{70} in small-scale experiments (m)	$2.08 \cdot 10^{-4}$
Gravitational acceleration (m^2/s)	9.81
Unit weight of submerged particles (kN/m^3)	16.5

Although the proposed model does not sufficiently cover the piping process, it has led to the development of several finite element models to assess dike safety due to BEP (van Esch, 2014; Robbins and van Beek, 2015). These will be further discussed in the following sections.

3.2 D-GEO FLOW AND GEOLIB

As previously mentioned, due to the change to the Dutch safety standards, piping and other geotechnical failure mechanisms have become highly important. In turn, more advanced and precise piping calculations had to be carried out. This led to the development of Deltares' finite element piping analysis tool called D-Geo Flow. Finite element method (FEM) is a numerical technique for solving partial differential equations. This procedure allows to obtain the evolution in space and time of one or more variables representing the behaviour of a physical system (Oñate et al., 2008). Since natural processes, such as underground water flow can, in many cases, be described by partial differential equations, FEM has become an essential tool to explore complex real-world situations such as piping, which would be otherwise impossible to solve analytically. D-Geo Flow is based on Sellmeijer's model but assesses

piping in a much more complete way by incorporating other effects like time-dependent hydraulic loads and heterogeneity of the subsoil (van Esch, 2014).

D-Geo flow carries out three different computations including the groundwater flow, the water flow in the erosion channel and the state of limit equilibrium of the particles at the bottom of the channel (Stoop, 2018). The software divides the element into a finite number of triangular elements. It then employs algebraic equations in which the unknowns are heads at nodal points of the triangles. The values within the elements are then interpolated from the nodal values using shape functions (Stoop, 2018).

While the D-Geo Flow platform is user-friendly, to perform a more detailed study of piping it can be combined with the GEOLib Python interface. This is a Python package including different models for several types of calculations regarding dike safety. Piping calculations can be made using the D-Geo Flow class in the package which is essentially interfaced with the D-Geo Flow module. However, GEOLib offers more ease in the customization of the project making it possible to adapt to more specific requirements, such as easily modifying the permeability of soil layers or creating complicated layer geometries. The ability to easily modify soil parameters and adjust the soil layers are the main reasons to select D-Geo Flow and incorporate the use of GEOLib.

3.3 DESICCATION CRACKS' EFFECT ON SOIL PROPERTIES

Desiccation cracks affect certain soil parameters and behaviours to different degrees one of the most reported effects of desiccation cracks on soil is the increase in the element's hydraulic conductivity. This property describes a material's ability to let water through and is defined in terms of volume per area and time (Musa and Gupta, 2019). Several studies have been carried out to better understand and quantify the effects and have been summarized in Table 2.

Table 2. Ratios of hydraulic conductivity increase found in the literature

Source	Ratio of hydraulic conductivity increase	Description of the study
Omidi et al. (1996)	1.25 to 11.29	Tested the hydraulic conductivity of 4 different soils.
Rayhani et al. (2007)	12.52 to 34.88	Studied 4 natural clayey soils from Iran.
He et al. (2015)	25	Tested natural clay with initial hydraulic conductivity in the order of 10^{-6} cm/s from Wuhan.
Albrecht and Benson (2001)	5 to 500	Subjected several soil specimens to hydraulic conductivity testing after cycles of drying and wetting.

While ratios are varied, all studies found a correlation between the generation of desiccation cracks and an increase in hydraulic conductivity.

Furthermore, the acceleration of infiltration due to desiccation cracking makes them highly dangerous for geotechnical structures. Several reports have found a high correlation between desiccation cracking and the initiation of soil piping (Foster et al., 2000, Parker and Jenne, 1967, Bernatek-Jakiel and Poesen, 2018). By allowing for easy penetration of water into the soil layers erosion pathways are formed which exacerbate the probability of piping failure (Foster et al., 2000). According to Bernatek-Jakiel and Poesen (2018), soils with swelling clays are especially prone to this phenomenon.

In addition, the generation of cracks has been associated with the reduction of erosion resistance of soil specimens. According to Jalil et al. (2020), low moisture levels lead to desiccation which will increase the hydraulic conductivity in turn reducing the resistance to internal erosion. This might not be significantly dangerous during drought periods since the water levels will be low. However, it is especially dangerous once the structure is exposed to high hydraulic heads, e.g., during a short period of heavy precipitation, since the subsequent seepage and the presence of existing cracks are very likely to cause internal erosion (Jalil et al., 2023).

In summary, desiccation cracks have multiple effects on the soil layer making them complicated to model. The main aspects that will be considered in the thesis are the increase in hydraulic conductivity and the fissures themselves which allow for more fluid penetration through the blanket layer. The decrease in erosion resistance and the swell-shrinkage behaviour mentioned in Section 2.3 will not be taken into consideration due to the complexity they involve.

3.4 DESICCATION CRACKS' GEOMETRICAL FEATURES

The main features which can be considered for the modelling of 2D desiccation cracks are the aperture, depths, and spacing. Nevertheless, as established by Khandelwal (2011) the existing models for the simulation of crack geometry are too specific to implement. In turn, the study made by Khandelwal (2011) will be used to establish the geometry of the fissures. In his thesis, he generated probability distribution functions for depths, spacing and aperture for individual cracks based on empirical values established in the literature. He sampled 4000 random values. According to his findings, all the variables listed follow a lognormal distribution. This probability distribution is represented by the following function:

$$f(x) = \frac{1}{x\sigma\sqrt{2\pi}} e^{-\frac{1}{2}\left(\frac{\ln(x)-\mu}{\sigma}\right)^2}$$

Where:

σ – standard deviation

μ – mean

In the case of spacing the mean is equal to 4.1964 cm while the standard deviation is 0.906 cm with a mode of 60cm. It is important to note that crack spacing was restricted to a maximum of 7m. The cumulative distribution function compared with the empirical distribution can be seen in Figure 6.

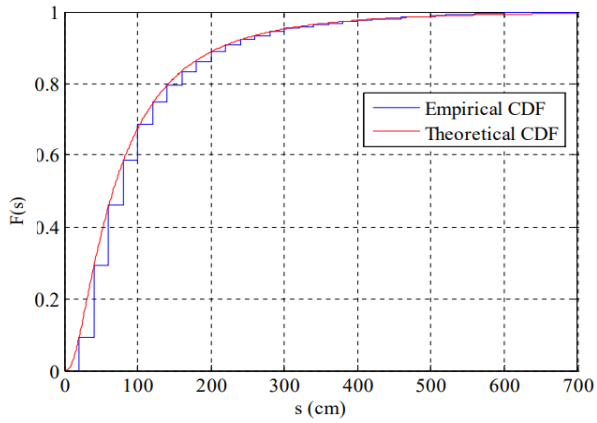

Figure 6. Cumulative distribution function graph for crack spacing (Khandelwal, 2011)

For the aperture, the mean is -4.4607m while the standard deviation is 0.5973. The values were restricted between 0.001 and 0.03m and the mode resulted in 0.008m or 0.8cm.

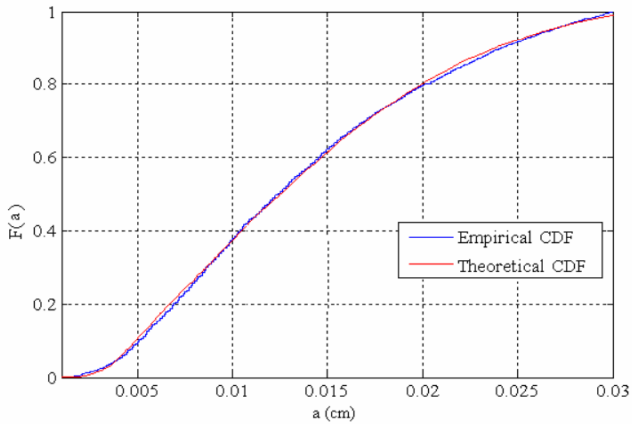

Figure 7. Cumulative distribution function graph for crack aperture (Khandelwal, 2011)

Finally, for crack depths, the mean is 4.3354 cm, and the standard deviation is 0.5793 cm. For this variable, the values were restricted to a maximum of 2m, and the mode was 60cm. The cumulative distribution function can be seen in Figure 8.

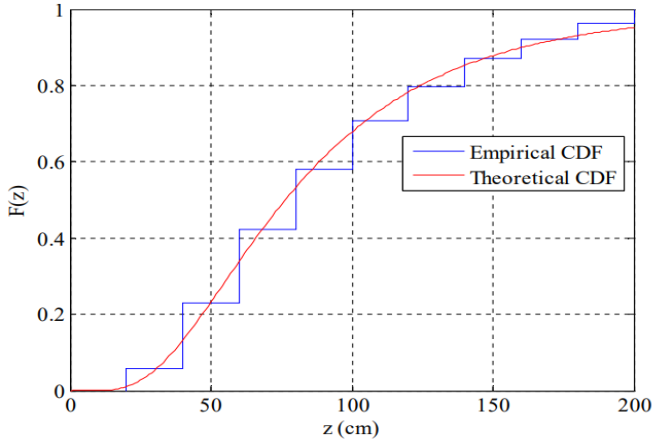

Figure 8. Cumulative distribution function graph for crack depth (Khandelwal, 2011)

In brief, the main features of desiccation cracks are depth, spacing, and aperture. All these variables follow a lognormal distribution function. The modes are 60cm, 60cm, and 0.8cm respectively. These probability distribution functions will be used to include stochasticity into the model to better represent reality. In the following, details on how these main features are incorporated into a numerical FEM model using the D-Geo Flow software will be presented.

4. NUMERICAL MODEL

4.1 STRUCTURE OF THE ANALYSIS

To determine the impact of desiccation cracks on failure due to BEP this study employs a systematic approach revolving around the development of a numerical model and testing of several scenarios. The methodology involves several steps to ensure the accuracy and relevance of the findings.

The initial step consists of the development of a Python script utilizing GEOLib which as previously explained is essentially interfaced to the D-Geo Flow module. The code allows for an easy setup of the geometry, characteristics and desiccation cracks layout, which facilitates running calculations regarding piping. The model will be based on a standard dike configuration defined by Stoop (2018) which integrates various piping-sensitive dike cross-sections. This dike geometry has already been verified and in turn, provides an ideal setup for the base model. Nevertheless, some minor changes have been undertaken and in turn, a verification will be done. A brief explanation of the verification will be given in a later section.

Using the verified model as the base, adjustments will later be made to include desiccation cracks and the corresponding changes in hydraulic conductivity in the blanket layer. Subsequently, various cases will be studied in which certain features will be altered including:

- Case 1: Modifying the number of cracks
- Case 2: Limiting the spacing between cracks
- Case 3: Limiting the aperture of cracks
- Case 4: Increasing the hydraulic conductivity of the cracked section

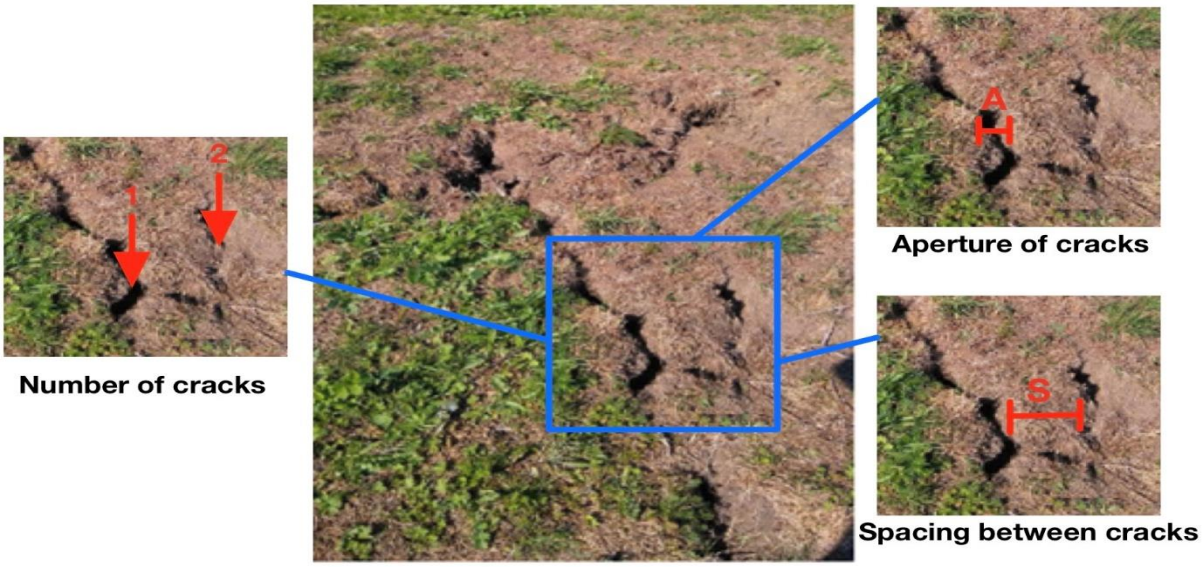

Figure 9. Modified features for the studied cases in a real-life context

Case 1 will study the effect of the degree of cracking of the blanket layer on the critical head. For this case, simulations will be run varying the number of cracks as well as considering the uncracked equivalent of the scenarios. This will allow to better understand not only how the presence of fissures affects failure due to BEP but also study the effect of the quantity of fissures. Case 2 will vary the spacing between cracks while case 3 studies the effect of the aperture of fissures by studying the effect on the critical head. These features can be seen in a real-life context in Figure 9. Finally, Case 4 will vary the hydraulic conductivity of the cracked section based on the ratios presented in Table 2.

The results obtained from the studied cases will assist in addressing the sub-questions proposed at the beginning of this thesis. By following this systematic approach, this thesis ensures a comprehensive analysis of the effects brought by desiccation cracks on the critical head.

4.2 BASE MODEL SETUP

4.2.1 Geometry

As previously mentioned, the base model is based on a standard cross-section established by Stoop (2018). The geometry is based on the mean dimensions from various geometries extracted from the HKV 'profielengenerator' which employs real-dike geometries based on the 'Actueel Hoogtebestand Nederland'. Stoop (2018) filtered the geometries to only include the ones located in a piping-sensitive region and which do not present relatively wide inland berm and wide foreshore due to the reduction of the probability of BEP it would generate. The dimensions of the dike have been approximately derived from the mean geometry in Figure 10.

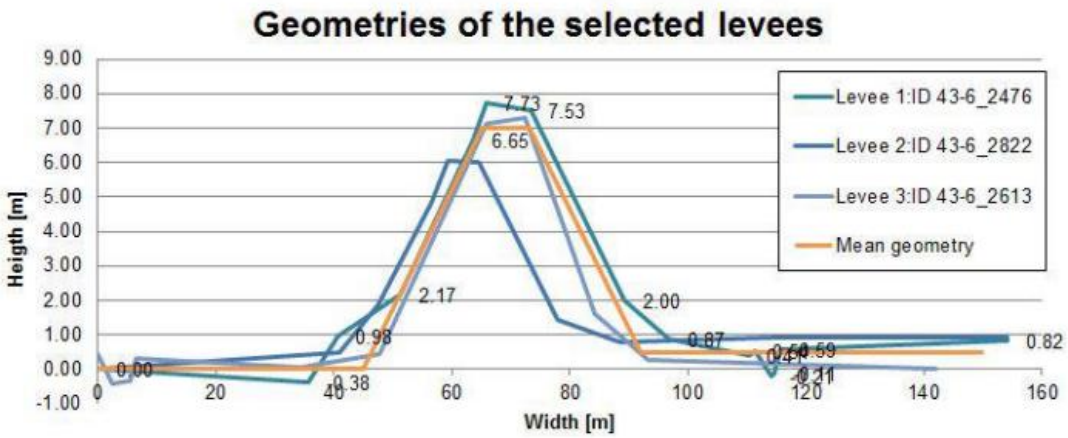

Figure 10. Generated geometries for selected levees (Stoop, 2018)

The cross-section is made up of three different layers including an impermeable blanket on the landside, a clay levee, and the permeable sand aquifer at the bottom. The depth of the aquifer influences the piping process since larger depths allow for a larger flow area (Stoop, 2018). In turn, a depth of 30 meters is considered for the base model to be able to run a proper analysis of the critical head.

As mentioned before BEP starts with the appearance of an unfiltered crack for flow to concentrate towards the surface. According to van Beek (2019), in D-Geo Flow one could model the defect as a gap in the blanket layer without head loss if a steady-state flow assessment of pipe progression is being carried out and the blanket layer is not too thin and permeable. It is also mentioned that the 0.3d rule which considers the resistance of fluidized sand in the exit channel, can be ignored in these cases. For this thesis, the latest version of D-Geo Flow is being used. This version does not consider changes in groundwater storage meaning all assessments are steady state (van der Meij, 2023). Additionally, the blanket layer will be made of highly impermeable material. As a result, in the base model, the gap in the blanket layer is designed as a ditch located at the toe of the dike with the dimensions stipulated by Stoop (2018) and without considering the 0.3d rule.

The final dimensions for the dike's cross-section are seen in Table 3 while the D-Geo Flow model geometry can be seen in Figure 11.

Table 3. Dimensions of base model layers

Dimensions	Value (m)
Aquifer height	30
Aquifer length	150
Levee height	7
Levee bottom length	47
Levee upper length	8
Blanket height	0.5
Blanket length	58
Ditch height	0.5
Ditch bottom length	0.1
Ditch upper length	0.3

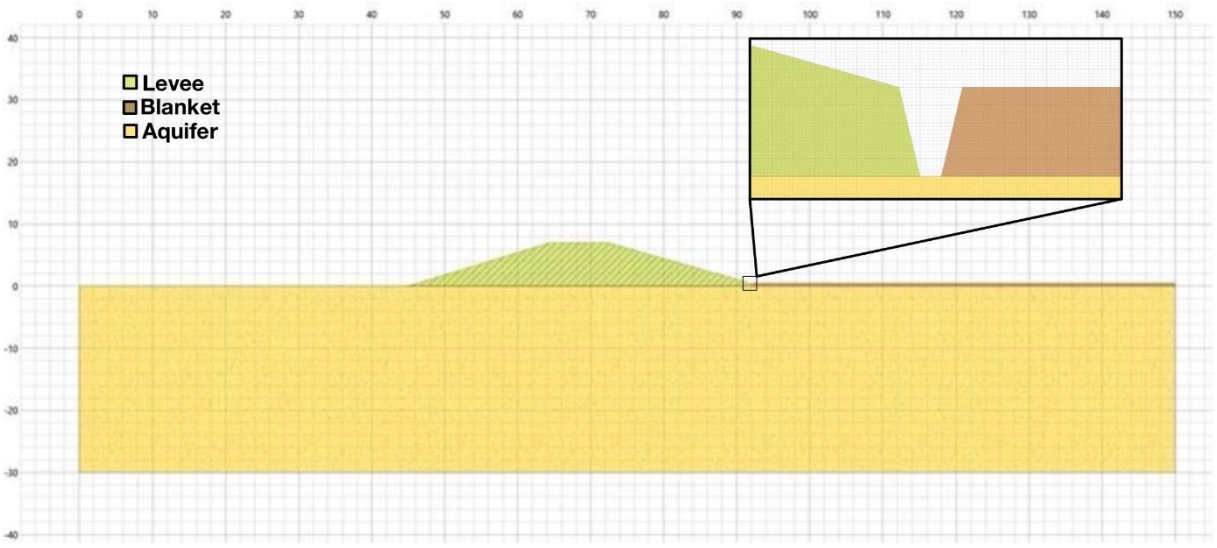

Figure 11. Final Geometry of the base model with a zoom-in on the ditch (yellow: aquifer, green: levee, brown: blanket)

It is important to note that Stoop (2018) used the addition of boreholes in D-Geo Flow to generate the cross-section. As mentioned, the geometry of this thesis model will be made through GEOLib, nevertheless, no major changes should be expected from this difference in construction methods.

4.2.2 Material Properties

The soil properties that will be used for the base model are again based on the verified model by Stoop (2018). These values are entirely based on his extensive research into different soil properties. Nevertheless, in D-Geo Flow the only soil properties that can be modified are the vertical and horizontal permeabilities. In this thesis, however, the materials used are not considered anisotropic and will have the same permeability for both directions. The values can be seen in Table 4.

Table 4. Hydraulic conductivity values in the base model

Layer	Hydraulic Conductivity (m/d)
Levee	0.01
Blanket	0.002

These values are low to maintain highly impermeable layers. Nevertheless, it is important to acknowledge these properties are not considered in the Sellmeijer calculations, since the adapted Sellmeijer rule only considers the soil under the dike's body. Since the aquifer's hydraulic conductivity and grain size are the main soil properties considered by Sellmeijer, they will be adjusted in the simulations to verify the base FEM model.

4.2.3 Boundary Conditions

For the model to properly reflect the physical constraints and behaviours of the system being studied certain boundary conditions must be set. In the model, water boundaries have been represented using fixed head boundaries since it is the only modification allowed by the current D-Geo Flow software (van der Meij, 2023).

It is also important to note by default D-Geo flow sets all outer boundaries as closed boundaries which refer to no flow boundaries through which water is not allowed to pass. The boundaries between layers however are open boundaries which do allow water flow. This cannot be modified.

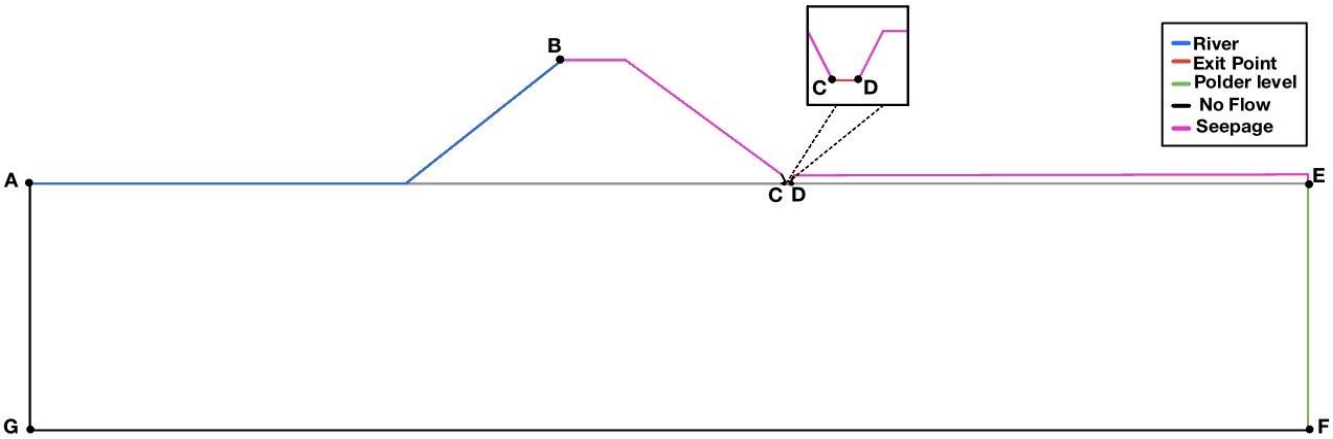

Figure 12. Boundary conditions for the base model (not to scale)

The boundaries AG and AF shown in Figure 12 are maintained in the default settings of no flow boundaries established by the program. The CD boundary will have a constant head of zero to consider for groundwater to flow out through the exit point. At the EF boundary, it is assumed the body of water is at rest, so there will be hydrostatic pressure created by a constant head equal to zero (Stoop, 2018).

The BC and DE boundaries are seepage boundaries between the saturated layer and the atmosphere defined by heads equal to the elevation head (Franke *et al.* 1987). Nevertheless, since the current D-Geo Flow version only allows for fixed head boundaries, a seepage boundary is not an option. In turn for the base model, the BC and DE boundaries are left by default as closed boundaries. It is also important to note that due to the impermeability of the layers beneath these boundaries, seepage at the surface will not occur (Stoop, 2018), further justifying the use of the no-flow boundaries.

The AB boundary is the boundary between the river and the levee. Stoop (2018) set this as a specified head boundary, which he mentions is specified as a function of position and time. While previous versions of D-Geo allowed this, in the current version modifying the river water level curve is not possible. In the current version the alternative is to set the AB boundary as a fixed head boundary and when running the critical head calculation set it as the critical head boundary. D-Geo Flow will then progressively increase the head in this boundary considering a user-inputted step size until the critical head is reached. In turn, the AB boundary is set as a fixed head boundary and selected as the critical head boundary for the calculations.

As can be noticed, the boundary conditions are where the base model and the model established by Stoop (2018) differ the most. This is mostly due to the differences in the version of D-Geo Flow used. As a result, it has been decided to run a verification on the base model instead of just assuming it is verified since it is based on the model by Stoop (2018).

4.3 VERIFICATION OF BASE MODEL

The verification of the model is done using the procedure proposed by Stoop (2018). The verification consists of comparing the critical head obtained from the model and the results from the adapted rule of

Sellmeijer. The different calculations are tested changing the values for the grain size and the hydraulic conductivity of the aquifer. The differences between the model and the Sellmeijer rule are obtained and presented in meters and as a percentage in Table 5. The aim is to maintain an average difference like the one reported by Stoop (2018) since his model is already verified.

The mesh size for the calculations has been established at 2m. This size was chosen to provide sufficient accuracy while still maintaining relatively low computation times. The pipe element size was maintained at 1m which is the default value in D-Geo Flow. Similarly, the step size at which the hydraulic head will increase is maintained at the default value of 0.1m, which allows for sufficient accuracy and relatively low run times.

Additionally, to run a critical head calculation in D-Geo Flow, search boundaries must be established. This means setting the range of hydraulic head values that the software will examine to find the critical head. The search boundary (AB in Figure 12) in the FEM model is set with a low of 0m and a high of 7m to search within the height of the levee, which is considered a realistic range.

Finally, the values for the pipe length and aquifer height are obtained from the proposed cross-section of the FEM model. These will be 47m and 30m respectively.

Table 5. Verification of base model

Scenario	d70 (m)	K (m/d)	Adapted Sellmeijer (m)	D-Geo Flow (m)	Diff (m)	Diff (%)
1	0,0003	3	6,25	6,5	0,25	3,846154
2	0,0002	5	4,48	4,7	0,22	4,680851
3	0,0002	10	3,55	3,7	0,15	4,054054
4	0,0004	10	4,69	4,9	0,21	4,285714
5	0,0001	2	4,61	4,8	0,19	3,958333
6	0,0001	10	2,69	2,8	0,11	3,928571
7	0,0001	1	5,8	6,1	0,3	4,918033
8	0,0008	25	4,56	4,8	0,24	5
9	0,0003	5	5,27	5,5	0,23	4,181818
10	0,0003	25	3,08	3,2	0,12	3,75
				Average	**0,202**	**4,260353**

As seen in Table 5 the average difference between the Sellmeijer rule and the base model is approximately 0.20m or around 4%. These are relatively low values, showing the model satisfactorily corresponds to the Sellmeijer rule. Stoop (2018) presented average differences of 0.15m or 5%. Since the values are like the ones obtained for a verified model, the base model is assumed to be sufficiently accurate.

4.4 CRACKED MODEL SETUP

Once the base model has been verified and deemed sufficiently accurate the next step is to modify it to include desiccation cracks. As previously stated, desiccation cracks are a natural phenomenon difficult to properly predict and simulate. In turn, only a small number of features will be considered in the model, namely the cracks' apertures, spacing, location and effect on the blanket's hydraulic conductivity. Stochasticity will be considered using probability distribution functions for the different features. This section will further explain the setup of the cracked model.

4.4.1 Crack Location

It is important to note that the cracks will be generated within only a specific section of the blanket. This section must comply with two main requirements:

1. Not being too far away from the dike's toe
2. Provide enough space for various cracks

The first requirement is necessary because if cracks were too far into the hinterland the results would not be relevant since failure of the dike would be highly unlikely. Regarding the second requirement the section needed to be large enough to fit various cracks to be able to study the effect of different number of cracks on the critical head.

As a result, it was decided that the cracks would be only generated within 5m of the dike's toe, as seen in the red area in Figure 13. This section provides enough space for various cracks as well as being close enough to the toe not to yield extremely high critical head values.

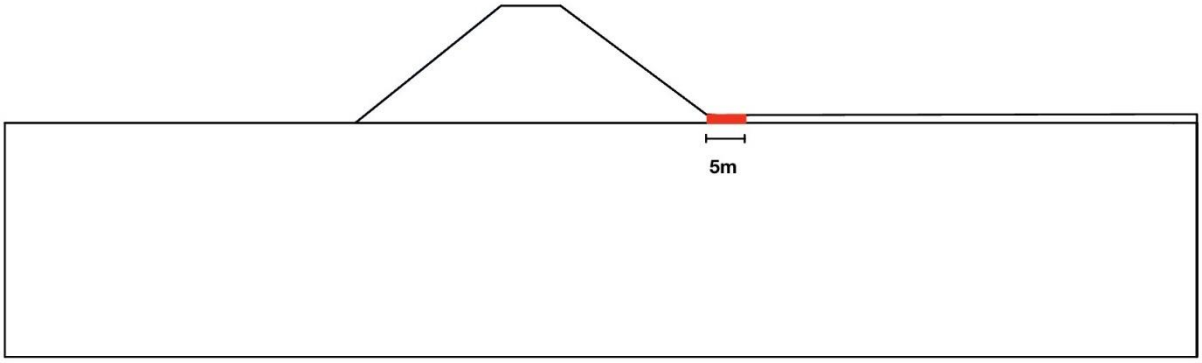

Figure 13. Section where cracks can be generated in the cracked model

4.4.2 Crack Geometry

The geometry of the cracked model will be overall like the base model. While the levee body and the aquifer remain the same, the blanket layer geometry will change to incorporate the new fissures. In addition, the ditch which served as the exit point for the base model will be removed since the new exit point will be one of the cracks.

The desiccation cracks will be modelled in a "V-shape" geometry, under the assumption they are symmetrical. In turn, each crack will have three coordinate points, the start, the middle and the end that will be used in D-Geo Flow to define the defects.

The aperture and the spacing of the cracks will be determined by using the lognormal distribution functions mentioned in Section 3.4. Nevertheless, while the depth can also be randomly generated utilizing a probability distribution function, a constant depth has been preferred since in D-Geo Flow the pipe trajectory has to be horizontal. In turn, if a crack is not as deep as the blanket layer, the pipe trajectory would need to be inclined which is not possible. As a result, the depth was established as 0.5m for all cracks.

An example of the desiccation cracks in the D-Geo Flow model can be seen in Figure 14.

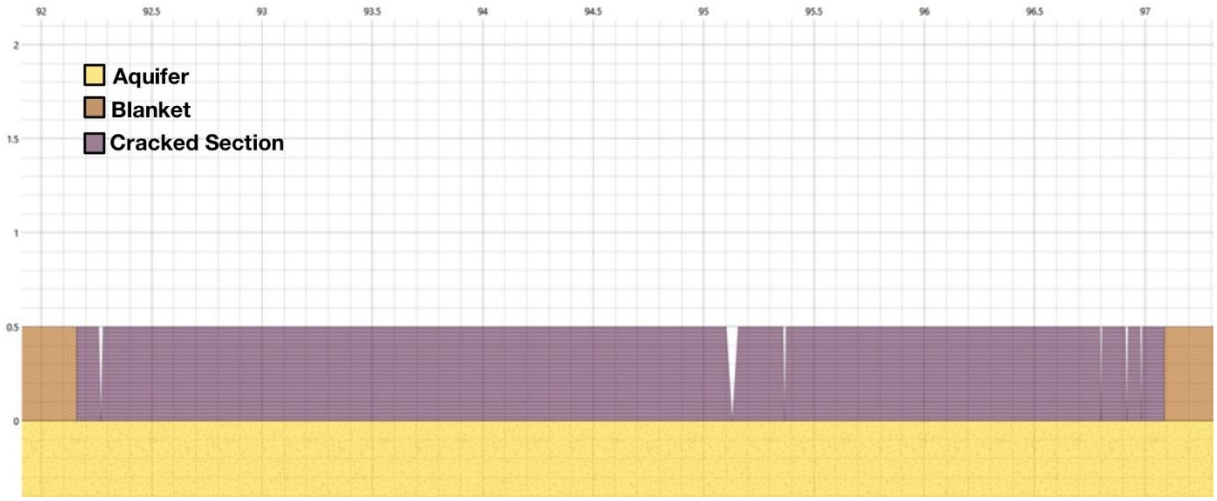

Figure 14. Example of cracks in the FEM model (purple: cracked section, brown: blanket layer, yellow: aquifer)

4.4.3 Change in Hydraulic Conductivity

Furthermore, as previously discussed, desiccation cracks have been attributed to an increase in the soil's hydraulic conductivity. In the base model, the hydraulic conductivity of the blanket layer is maintained at 0.002 m/day or 2.31×10^{-6} cm/s. This will be taken as the initial hydraulic conductivity and will be increased based on ratios discussed in section 3.3.

The change in hydraulic conductivity will be implemented in the model only in the cracked section of the blanket layer. This section is assumed to extend from 0.1m before the first crack until 0.1m behind the last crack. The cracked section can be seen in purple in Figure 14.

4.4.4 Boundary Conditions

As with the geometry, the boundary conditions used for the cracked model will be almost the same as the ones implemented for the base model. The only boundary that was modified is the exit point boundary. This remained as a fixed head boundary with a value of zero. However, since cracks are the exit points and not the ditch then the boundary is applied to the cracks. It will be implemented from the start point till the end point of the fissure as seen in Figure 15. Nevertheless, since there can only be one exit point per calculation, the boundary will vary per crack depending on which defect is being considered as the exit point, and the rest of the cracks will possess the default closed boundary set by D-Geo Flow.

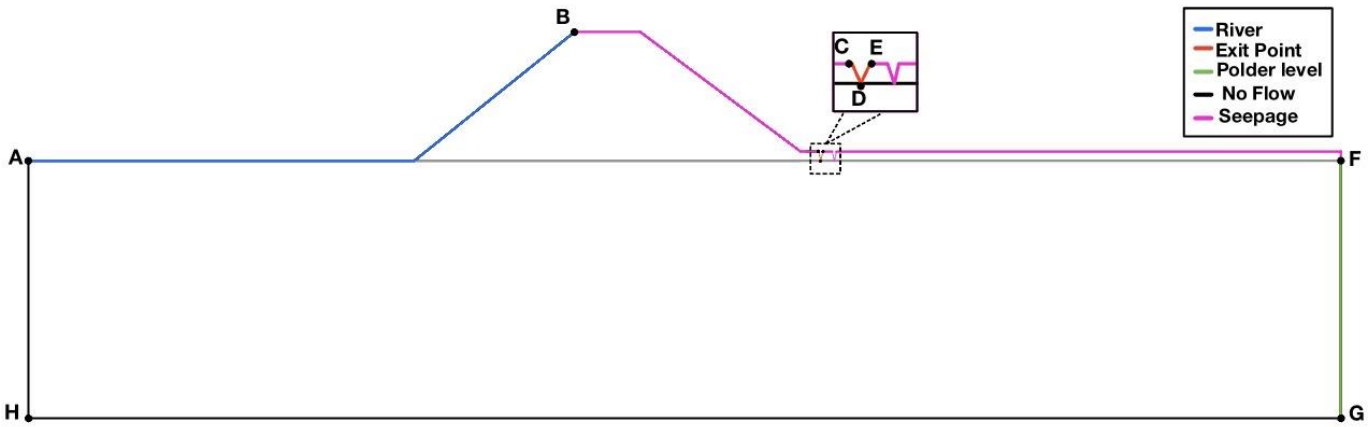

Figure 15. Boundary conditions for the cracked model

4.4.5 Material Properties

For the verification of the base model the critical head was calculated employing several combinations of the aquifer's hydraulic conductivity and d70 values and the results were compared with the adapted Sellmeijer rule. From these combinations, the one that presented the lowest percentual difference with the rule used values of 0.3mm for d70 and 25m/d for the hydraulic conductivity. Consequently, these values will be used for the cracked model's aquifer.

The hydraulic conductivity of the dike's body will remain the same with a value of 0.01m/d. The blanket layer section which does not include cracks will also maintain its hydraulic conductivity equal to 0.002m/d.

Table 6. Soil properties in the cracked model

Layer	Hydraulic conductivity (m/d)	D70 (mm)
Blanket	25	0.3
Levee	0.01	-
Aquifer	0.002	-

4.4.6 Cracked Model Generation

The generation of the cracks is a systematic process which starts with the user setting the number of cracks desired in the model. Subsequently, an initial crack is generated. The location of the crack is chosen based on a uniform probability distribution function, meaning that all the locations within the first 5m of the blanket have the same probability of developing a fissure. The aperture for this crack is randomly generated using the lognormal distribution function mentioned in section 3.4. Once the initial crack is set, the script will randomly choose if the next crack shall be in front or behind the initial one. Once this choice has been made the aperture and spacing between the cracks will be established using the lognormal distribution functions previously mentioned. Considering this spacing, if the location of the crack is within the 5m section, the crack will be generated, if not the process will be done again until the crack is located within the specified section. This process will continue until the number of required cracks is met.

The generation of the cracks essentially refers to the generation of the start, mid, and end point coordinates. Once these points have been obtained, they can be used in combination with GEOLib functions to set the cross-section, establish the boundary conditions and determine the pipe trajectory. Once everything has been set, the GEOLib functions will allow for the information to be transferred to D-Geo Flow to make the necessary calculations and yield a result. A simplified flowchart of the process can be seen in Figure 16.

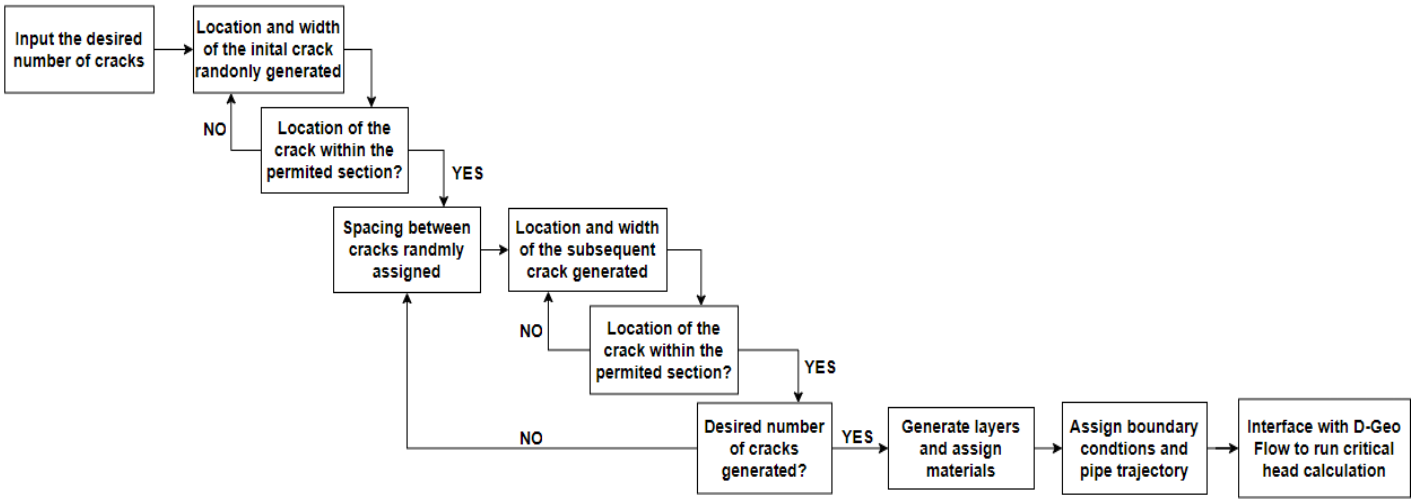

Figure 16. Flowchart of the cracked model generation process

It is important to emphasize this is just a brief explanation of the created Python script and how it works to generate the model and obtain a result. Nevertheless, for a more detailed look, the code can be accessed via this link which is also found in Appendix D.

5. SETUP OF THE CASES

This section will present a more in-depth explanation of the numerical simulations and how they will be setup and carried out. Firstly, the model parameters that will be used for all the assessments will be established.

The step size at which the hydraulic head will increase will be lower compared to the one used for the verification. The adopted value for the numerical simulations will be 0.01m. This setup will allow to obtain a more accurate critical head while maintaining an acceptable computational time. The search boundaries will remain with a lower head level of 0m and a higher head level equal to 7m.

Furthermore, since the space between cracks can be relatively small a large mesh could lead to inaccurate results. In turn the mesh size for the cracked layer will be reduced to 0.2m. The final mesh sizes per layer are specified in Table 7 and seen in Figure 17.

Table 7. Mesh sizes for the numerical simulations

Layer	Mesh size (m)
Levee	2
Aquifer	2
Blanket	2
Cracked Blanket	0.2

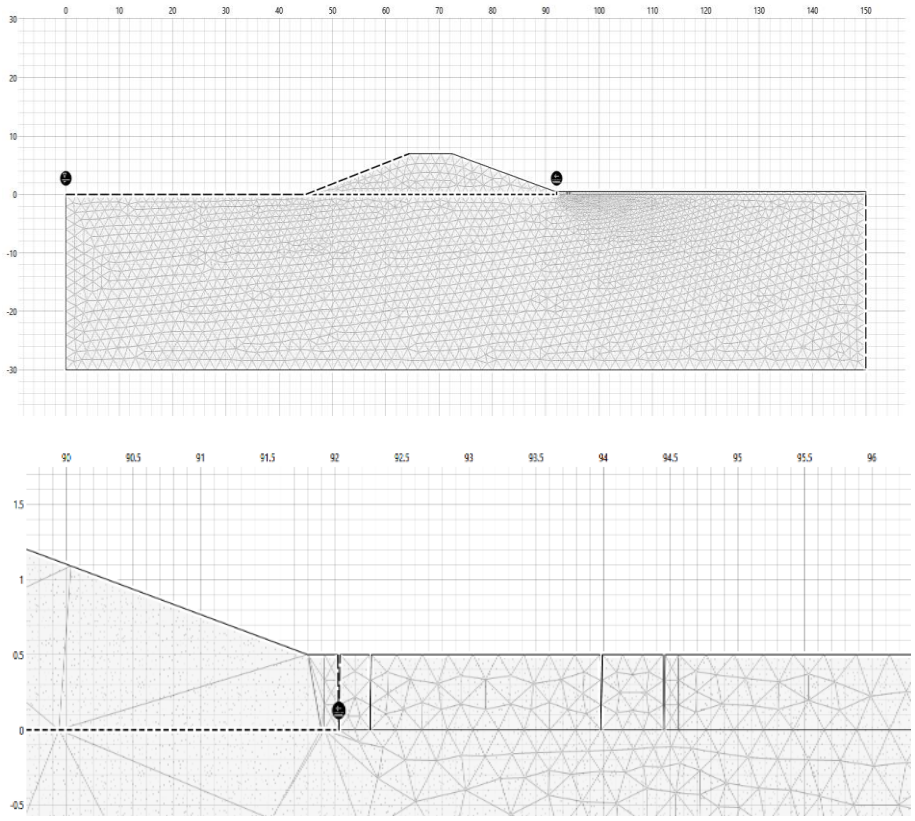

Figure 17. Mesh in D-Geo Flow (upper: mesh of the dike. lower: mesh in cracked section)

It is also important to note the hydraulic conductivity of the cracked section will be increased using a ratio of 25 regarding the initial blanket layer's value. This is based on the findings of He *et al.* (2015). The ratios proposed by other studies such as Albrecht and Benson (2001) and Omidi *et al.* (1996) presented very different initial hydraulic conductivities or very extreme ratios and in turn, were not considered. As a result, the hydraulic conductivity of the cracked section for Cases 1, 2 and 3 will be equal to 0.05 m/d. In Case 4 the value will be adjusted in every calculation.

For each case, the calculations conducted will be regarding the critical head. As previously mentioned, this is a good indicator when studying the probability of failure of a dike due to BEP and in turn, can aid in understanding the effect of desiccation cracking.

It is important to note that not all the desiccation crack geometry features discussed in Section 3.3 are considered. The effect of depth will not be studied since as previously mentioned this parameter will remain constant.

5.1 CASE 1

To better understand the degree to which cracks affect the critical head, a comparison will be made using an uncracked and a cracked model. The uncracked model will be the same as the cracked one except for two distinctions.

1. The uncracked model will not possess any defect in the blanket layer but instead have one uplift boundary per calculation placed at the location of one of the cracks which will act as the exit point.
2. Since it does not consider cracks, no adjustments to the hydraulic conductivity will be made.

The uplift boundary will have a constant head to represent the pressure needed to achieve uplift conditions and consider the initiation phase of the piping mechanism. The calculations to determine this pressure will be discussed later. For further information regarding this model, the script can be accessed through the link in Appendix D. Additionally, various scenarios will be run to consider the different number of cracks and be able to analyse the effect on the critical head.

Since it is not known which crack will be the exit point in reality, the comparison will be made considering ranges for the critical head instead of specific values. These ranges will be obtained by calculating the critical head using the first and last crack since these situations will yield the minimum and maximum values for each scenario. For example, for a scenario of 2 cracks four critical head calculations would be run and the setups can be seen in Figure 18.

1. The first calculation would be done with the crack model using the first crack as the exit point. Here the change in hydraulic conductivity and all the cracks are considered. As seen in the first case in Figure 18.
2. The second calculation will be the same as the first but with the second crack as the exit point, as seen in the second case in Figure 18.
3. For the third calculation, the uncracked model would be used where the uplift boundary would be set in the location of the first crack with a width equal to the first crack's aperture. For this scenario, the uplift boundary is the exit point. Since the blanket is not cracked an increase in hydraulic conductivity is not considered. This is represented in case 3 of Figure 18.
4. The fourth calculation would be the same as the previous one but considering the location of the second crack which can be seen in case 4 in Figure 18.
5. The ranges will be constructed based on the critical heads obtained from the calculations of both models and will then be used to compare the situation with fissures and without. To consider the stochasticity of the model, the scenarios will be run 6 times each. From these runs an average of the ranges will be obtained that better represents reality than just running the model once.

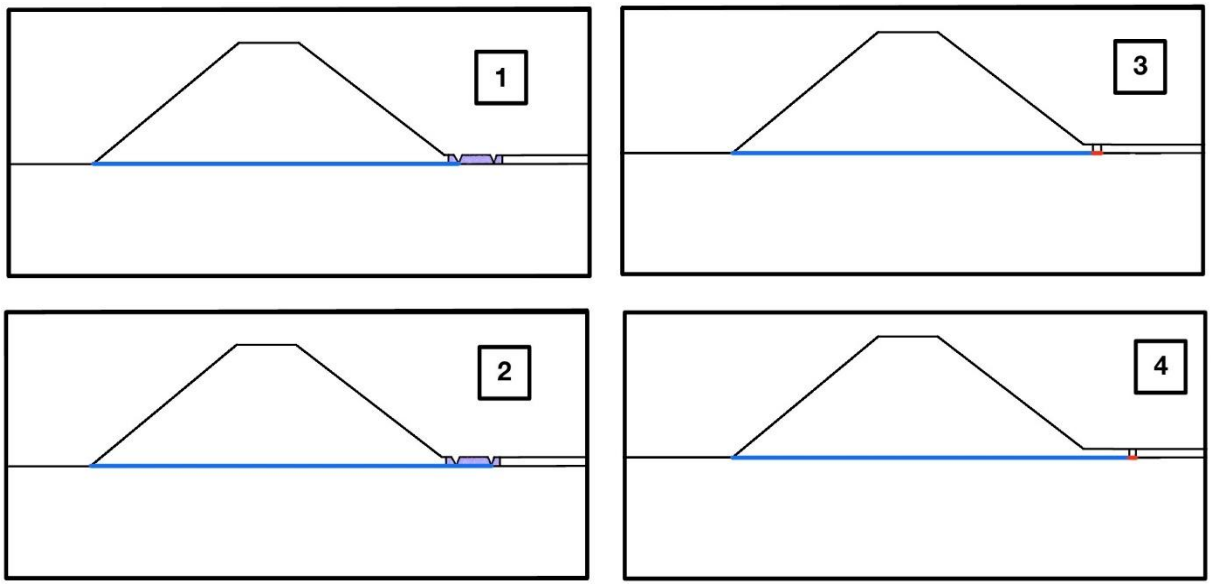

Figure 18. Example of calculations made for 2 crack scenario (blue: pipe trajectory, red: uplift boundary, purple: section with increased hydraulic conductivity) (not to scale)

5.1.1 Uplift Boundary

As mentioned in the literature review the initiation phase for the piping mechanism starts with the presence of a defect in the blanket layer. In certain cases, this defect can already be present, for instance

in the case of desiccation cracks. Nevertheless, in the cases where the defect is not present the blanket layer must be cracked. If the water pressure underneath the blanket layer exceeds the weight of the blanket itself uplift and rupture will follow (van Esch, 2014; van Woudenberg, 2023). In turn, the uplift boundary will represent a limit where if the water pressure needed for uplift is met the piping process can be initiated, if the condition is not met the mechanism will not start. However, a pressure cannot be applied in the D-Geo Flow model and in turn a head representing this pressure shall be obtained and applied to the boundary. The following calculation has been carried out to obtain said head.

First, the weight per meter of the section which is being considered for the uplift boundary shall be computed:

$$\gamma * b * h = w\ [kN/m]$$

Where:

γ – unit weight of clay (20 kN/m^3)

b – aperture of the crack (m)

h – height of the crack layer (m)

Subsequently, the pressure to lift this weight is obtained:

$$\left(\frac{w}{b} * 1000\right) = P\ [Pa]$$

Finally, the head is obtained:

$$\frac{P}{\rho g} = h\ [m]$$

Where:

ρ – density of water (1000 kg/m^3)

g – gravitational acceleration (9.81 m/s^2)

5.2 CASE 2

To test the effect of the spacing between cracks on dike failure due to piping, several calculations will be run with the cracked model. Each scenario will maintain a range of possible spacing. The limits for these ranges have been chosen based on the 25th (0.36m), 50th (0.60m), 75th (1.22m), and 90th (2.12m) percentile considering the lognormal probability distribution function used to determine the spacing. The bounds in turn will be 0-0.36, 0.36-0.60, 0.60-1.22, and 1.22-2.12.

The spacing will be limited to 2.12m since it is the 90th percentile and this is considered representative of what can be expected. Going beyond this would take into account spacings which have a low probability of happening. Additionally, it would be hard to include consistently large spacings in the model, since it is being considered cracks will appear within 5m from the toe of the dike. Furthermore, it is important to note that all the calculations will be run considering a setup of 4 cracks in the hinterland.

Since the model considers stochasticity through randomness in several parameters including spacing, the four scenarios will be run 6 times each to obtain an average of critical head ranges. The critical head ranges will be obtained as explained in the previous case. These ranges will then be compared with each other to determine the effect of spacing on the critical head.

Unlike Case 1 here no comparison will be made with the uncracked FEM model because the degree of cracking is not being tested but rather the effect of the cracks' features on the critical head. Since this also holds true for cases 3 and 4 the comparison with the uncracked situation will only be used for Case 1.

5.3 CASE 3

To analyse the effect of crack aperture on the probability of dike failure due to BEP a similar framework as with Case 2 will be employed. In this case, several scenarios will be run, using different ranges for aperture. Again, the ranges are based on the 25^{th} (0.008m), 50^{th} (0.012m), 75^{th} (0.017m), and 90^{th} (0.025m) percentile considering the lognormal probability distribution function used to determine the aperture.

In addition, to account for the stochasticity in the model 6 calculations will be run per scenario to obtain an average of the critical head ranges. The ranges will then be compared regarding the aperture.

5.4 CASE 4

To assess the impact of the increment in the hydraulic conductivity of the blanket section due to desiccation cracking, multiple simulations will be carried out. In each one, the hydraulic conductivity of the cracked layer will be adjusted considering different ratios of final hydraulic conductivity to initial (K_f/K_i). Nevertheless, all the other parameters of the model (i.e. location of the cracks or the hydraulic conductivity of the sand) will remain the same. The ratios were obtained from the literature and ranged from 1.25 to 500. The initial hydraulic conductivity of the blanket layer will be 0.002 m/d as in the base model. For each different hydraulic conductivity value, several calculations will be conducted to construct a range of critical heads. This range will be used to compare between scenarios.

6. RESULTS AND DISCUSSION

This section will present and discuss the results obtained from all the studied cases.

6.1 CASE 1

The results for the critical head ranges obtained from 4 different scenarios with varying number of cracks can be seen below.

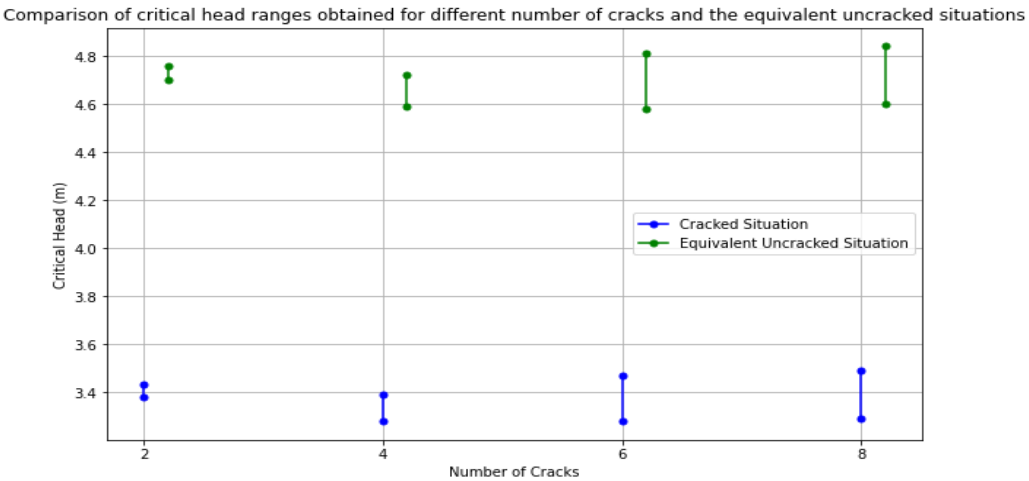

Figure 19. Comparison of critical head ranges for cracked and equivalent uncracked situations with varying number of fissures

Table 8. Difference between cracked and uncracked results

Number of cracks	Average difference between cracked and uncracked ($\Delta = H_{c,uncracked} - H_{c,cracked}$) (m)	Average percentual decrease difference $\left(\frac{\Delta}{H_{c,uncracked}} \cdot 100\right)$ (%)
2	1.33	28.05
4	1.32	28.38
6	1.32	28.14
8	1.33	28.14

Table 9. Span of critical head ranges for different number cracks

Number of cracks	Critical head range span for the cracked situation	Critical head range span for the equivalent uncracked situation
2	0.04	0.05
4	0.11	0.13
6	0.19	0.23
8	0.2	0.24

From Figure 19 it can be observed that the cracked model consistently presents a lower critical head range than that of the uncracked situation. Table 8 shows how the difference between the situations is on average around 1.32 to 1.33 meters or around a 28% decrease due to the cracks.

As stated by Bernatek-Jakiel and Poesen (2018) the initiation and occurrence of soil piping is correlated with periods of desiccation that lead to soil cracking. The presence of fissures provides a defect in the blanket layer which allows for an easier initiation of the piping mechanism since high hydraulic pressure in the aquifer is not needed to burst the blanket layer. This explains the consistently lower critical head ranges obtained from the cracked situation. The 28% decrease in the average critical head due to the presence of cracks in the hinterland leads to a higher probability of failure of the dike.

Additionally, the tests also show that the critical head range span or difference between the maximum and minimum critical head increases with the increase in the number of cracks. This trend can be seen in the cracked and uncracked situations. As shown in Table 9 the spans for the model considering desiccation cracks present relatively similar spans when compared to those yielded by the uncracked model.

The larger spans related to the higher number of cracks can be linked to the pipe length generated with every crack. Since there are more cracks to accommodate, the fissures tend to be more distributed leading to a larger difference between the location of the first and the last crack. In turn, the difference between the pipe trajectory length for the first and the last cracks are larger leading to a higher difference in the critical heads and a larger range span.

Finally, the results yielded no correlation between the number of cracks and the critical head. Figure 19 shows how there is an initial decrease in the minimum critical head from 2 to 4 cracks. However, the lower bound stayed relatively unchanged for 4, 6, and 8 fissures. For the higher bound of the ranges, the critical head decreases from 2 to 4 cracks but increases from 4 to 8 cracks. Furthermore, the higher critical head for scenarios with 2, 6 and 8 cracks, are approximately the same.

While the literature does suggest desiccation cracking leads to potential erosion pathways, the D-Geo Flow software only considers one pipe trajectory per calculation and in turn the number of cracks does not lead to a variation in the critical head. The variations in the critical head ranges are mostly due to the randomness assigned to the location of the cracks which ends up affecting the pipe trajectory length and in turn the critical head. This explains the absence of a correlation between the critical head and the number of cracks.

In summary, the presence of cracks increases the chance of BEP failure in dikes. In addition, the higher number of cracks allows for a higher number of exit points which leads to a larger range of hydraulic heads which can result in pipe propagation. Nevertheless, the number of cracks does not show any relation with the critical head and in turn the probability of failure of the dike.

6.2 CASE 2

The results obtained from the calculations can be seen in Figure 20 and Table 10. As previously mentioned apart from Case 1, the rest of the studied cases will not consider the uncracked FEM model, since the cracks' features effects are the parameters being tested and not the degree of cracking.

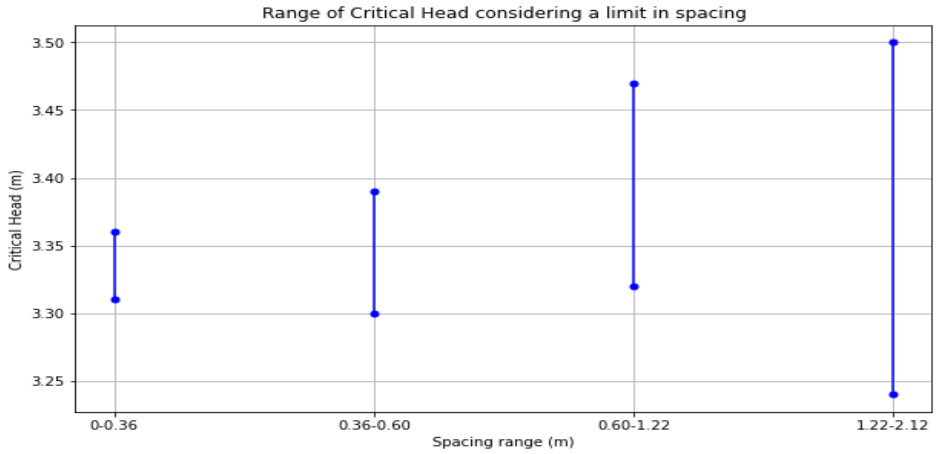

Figure 20. Comparison of critical head ranges with different spacing ranges

Table 10. Span for different spacing ranges

Spacing Range (m)	Critical Head Range Span (m)
0-0.36	0.048
0.36-0.6	0.087
0.6-1.22	0.150
1.22-2.12	0.262

From Figure 20 several observations can be observed. Firstly, it is evident the maximum critical head increases with the higher spacing. Nevertheless, the lower bound of the ranges is maintained approximately the same for the first three spacing ranges and relatively lower in the last scenario. Finally, the results also yield a correlation between the increased spacing and the span of the ranges, with larger spans being generated when the spacing is larger.

Regarding the relation between the upper bound of the critical head ranges and the spacing, the larger separation between fissures leads to the last crack being pushed further away from the dike. This will

lead to a larger pipe trajectory length which explains the larger critical head. With the lower bound, this is not the case, since the last scenario presents a relatively lower value. Since the spacing between 1.22 and 2.12 is relatively large, to fit all the cracks they must be spread out through almost the entire 5m being considered for the cracked section. As a result, the first crack is closer to the toe than in the rest of the scenarios, leading to a lower value for the lower bound.

Moreover, the correlation between the increased spacing and the expansion of the ranges' span can be attributed to the pipe trajectory length generated by the first and last cracks. When the separations between cracks are greater, the difference between the pipe lengths generated by the first and the last crack increases, in turn leading to a broader span for the critical head. The larger ranges related to the higher spacing suggest greater uncertainty in predicting the exact conditions under which BEP will happen, in turn, the dikes might need more robust safety standards to withstand the broader ranges.

In summary, the results show the main effect of crack spacing is on the pipe length. With higher spacing between cracks, the span of the ranges of critical heads will increase meaning the hydraulic head at which the dike will fail is more variable. In addition, it can be concluded that in the FEM with a spacing around 1.22 to 2.12 the cracks might start forming closer to the dike's toe leading to a lower critical head for the first crack compared to the other scenarios.

6.3 CASE 3

The results yielded by the calculations regarding the changes in aperture can be seen in Figure 21 and Table 11.

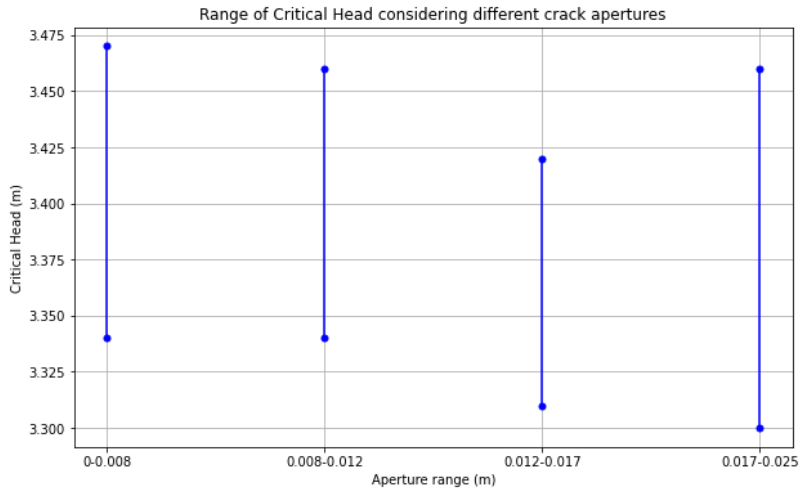

Figure 21. Comparison of critical head ranges with different aperture ranges

Table 11. Span for different aperture ranges

Aperture Range (m)	Critical Head Range Span (m)
0-0.008	0.13
0.008-0.012	0.12
0.012-0.017	0.11
0.017-0.025	0.15

The results show that the critical head ranges are highly similar throughout all the scenarios. While minor differences can be seen this accounts for distinctions of millimetres in the critical heads. In addition, the span of the ranges shows no correlation with the aperture increases. The spans remain similar throughout the four scenarios. The effects of the increases in the aperture on the critical head could be considered negligible since no distinctive changes were seen either in the critical head ranges or their spans.

Stoop (2018) alluded to how the exit point configuration has relatively small effects on the critical gradient. He mentioned changes of only 3% with exit points 50 times larger. Considering the changes in crack aperture are particularly small, this would explain why no extreme changes can be seen in either the critical head or the spans.

6.4 CASE 4

The results of the analysis on the effect of the increase in hydraulic conductivity due to desiccation cracking can be seen in Table 12.

Table 12. Critical head ranges for different hydraulic conductivities

Ratio (K_f/K_i)	Hydraulic Conductivity (m/d)	Critical Head Range
1.25	0.0025	3.24-3.38
11.29	0.023	3.24-3.38
25	0.05	3.24-3.38
34.88	0.068	3.24-3.38
500	1	3.24-3.38

As seen from the results the critical head remained constant. Additionally, it is important to observe that since the initial hydraulic conductivity of the layer was relatively low even with the increments the layer remained highly impermeable.

Stoop (2018) ran a sensitivity analysis regarding the blanket layer and the pipe development and concluded changes in the hydraulic conductivity of the layer produce negligible effects on the critical head. The study mentions that the ground water flow is dominated by the exit boundary and in turn this is one of the aspects of the model with more influence, leading to the low influence of the blanket layer parameters.

Since the crack section is in the blanket layer, changes in its hydraulic conductivity will also have insignificant ramifications on the model results. This explains the unchanged critical head obtained through all calculations in Case 4. To observe drastic changes in the critical head, the increase in the hydraulic conductivity would have to be enormous, effectively leading to an unrealistically high level of permeability for the clay blanket layer.

In summary, the hydraulic conductivity increase due to desiccation cracking in the blanket layer does not affect the critical head and as a result, does not yield any changes in the probability of failure due to BEP on dikes.

7. CONCLUSION

In this concluding section, the key findings from the research are summarized to address both the sub-questions and the main research question. The section begins by presenting a concise summary of the answers to the sub-questions. This is followed by a comprehensive answer to the main research question and finishing with an overall conclusion that captures the study's insights and implications.

1. Which characteristics of desiccation cracks should be considered when studying their effect on BEP and to what extent do they influence the propagation of pipes?

Desiccation cracks are a highly complex phenomenon involving a variety of characteristics and intricacies. Nevertheless, in a 2D setup three main geometrical fissure features can be distinguished which should be considered when studying BEP and desiccation cracking. These are crack depth, aperture, and spacing. Through these characteristics, a network of unique desiccation cracks can be represented which helps to better understand their effect on piping from a more realistic perspective.

Additionally, another important characteristic which should be considered is the effect of the fissures on the hydraulic conductivity of the soil layer. The cracks allow for an increased flow of water through the material, which translates into a higher hydraulic conductivity in a range of 1.25 to 500 times higher depending on several factors. This affects the soil's ability to resist internal erosion which is important in the study of BEP.

The degree to which spacing, aperture and the increase in hydraulic conductivity of the cracked section affect the propagation has been studied through Cases 2, 3 and 4 respectively. Regarding the crack aperture and the increase in hydraulic conductivity, no significant effect on the piping mechanism could be established based on the results obtained through the cracked model.

Concerning the effect of spacing, results showed that a higher value would lead to a larger span for the critical head range. This means the minimum and the maximum possible critical heads presented a higher difference with higher crack spacing. The larger span relates to a higher variability in possible critical heads meaning there are more possible hydraulic heads that will lead to the propagation of the pipes and connection of the upstream and downstream sections. In turn with higher spacing, there is more uncertainty regarding the exact conditions at which BEP will happen making more robust safety standards highly important.

2. How can the complexity of desiccation cracks be implemented into a model regarding BEP?

The complex nature of desiccation cracks makes them highly challenging to model. Nevertheless, the main geometrical features of the cracks have been used to account for certain stochasticity regarding the fissures and better understand their impact on BEP.

In this thesis, it was determined that to better represent reality, empirical data and probability distribution functions were the best way to consider the complexity of crack networks. Through the carried-out literature review, lognormal distribution functions for the aperture and spacing of cracks were discovered. These in combination with a uniform distribution function for the location of the cracks were implemented into a script to generate cracks which mirrored those present in reality. The script was then interfaced with D-Geo Flow via GEOLib to create a model which not only considers the complexities of desiccation crack geometry but also helps implement them into calculations regarding BEP.

3. To what extent is BEP influenced by the degree of cracking of the blanket layer?

The degree of cracking of the blanket layer was considered in Case 1 through both comparisons between cracked and uncracked situations and observations regarding the number of cracks. The results showed that cracking led to an average of 28% decrease in the critical head in reference to a situation with no fissures. This suggests that the presence of fissures leads to a higher probability of dike failure due to BEP.

In addition, the results from Case 1 also show the number of cracks does affect the critical head range span. With a higher number of cracks, there will be a larger variability in the critical head. While this does not mean there is a higher chance of failure, it does mean there is a larger range of hydraulic heads which can lead to pipe propagation from one side to the other of the dike body. Again, higher spans lead to higher uncertainty regarding the exact conditions at which BEP would occur, suggesting more cracks increase the uncertainty.

Furthermore, no relation between the critical head and the number of cracks was found, suggesting the decrease in the critical head due to cracks is mostly related to pipe initiation and not propagation.

In summary, the developed numerical model simplified the otherwise complex phenomenon of desiccation cracks through the use of empirical data and probability distribution functions regarding the fissure's geometrical features. This allowed to run several calculations considering distinct crack characteristics and effects to determine the implication on the BEP mechanism on clay river dikes. The results showed that while the crack aperture and the cracked layer's hydraulic conductivity do not impact the probability of failure due to BEP, the spacing and degree of cracking do.

In general, desiccation cracks lead to a higher probability of failure due to BEP. Their main effect is on the pipe initiation since fissures allow for preferential paths for fluid flow and avoid the need for high hydraulic heads to achieve uplift conditions. This is backed by the fact that cracks in the numerical model decreased the critical head by an average of 28%. In addition, the higher spacing and number of cracks led to a larger range of hydraulic heads which can lead to pipe propagation. Meaning there would be a higher uncertainty regarding the specific critical head at which a dike might fail.

In conclusion, it is considered that desiccation cracking highly affects the initiation of the BEP mechanism. However, the degree to which it affects the propagation of pipes is limited, as cracks primarily only add uncertainty to determining the exact critical head at which the dike could fail.

8. LIMITATIONS AND RECOMMENDATIONS

While this study provides valuable insights into the effects of desiccation cracking on the probability of failure due to BEP, it is important to acknowledge its limitations. For instance, the setup of certain parameters such as the grid size or the boundary conditions may limit the result of the simulations. Smaller mesh sizes would provide a more accurate result, nevertheless, this would be at the expense of the time to run the model. The negligible changes in Cases 3 and 4 could be directly linked to the fact that the mesh size was still too large. In addition, the Sellmeijer rule includes several parameters that are kept constant or cannot be translated directly from the FEM model, this could affect the comparison

between the critical heads obtained with the FEM model and the adapted Sellmeijer rule. For example, the Sellmeijer rule does not consider aspects such as the soil layers or the dike dimensions.

Furthermore, it is important to note the numerical model itself does possess certain limitations. Firstly, it was observed that the model does yield extremely high values for the critical head (over 7m) with certain configurations. While this error was not observed often, it is important to keep in mind when using the model. For this thesis, the critical heads over 7m were not considered as they are not realistic values.

Additionally, the inability of D-Geo Flow to consider pipe trajectories which are not straight lines limits the scenarios in which the model can be utilized. Finally, due to the stochasticity, the results from different calculations can vary considerably. This makes the comparability of results fairly difficult.

Despite the limitation and based on this thesis the use of the developed numerical model to study in a simplified way the relation between desiccation cracks and BEP can be recommended. Furthermore, to broaden the understanding of the mentioned phenomena the following various subjects can be further studied.

- Desiccation crack formation: This thesis did not consider the requirements for the formation of desiccation cracks in the blanket layer. In the future, a more elaborate modelling of the cracks can be undertaken to consider the soil conditions for crack formation and the more complex aspects of their development. Climate change scenarios, soil moisture, and swell-shrinkage cycles data could be used to enhance this analysis. This could lead to a more complete understanding of how desiccation cracks impact clay dikes and the climate resilience of these structures.
- Study of the effect of crack depth on BEP: Due to limitations regarding the pipe trajectory in D-Geo Flow the depth of the cracks was maintained constant. Nevertheless, it could be useful to study the effects of varying crack depths on the critical head. The analysis could aid in better understanding how the geometrical features of the fissures affect the probability of failure due to BEP.
- Different material soils: While the thesis focused on desiccation cracks on clay different soils could be studied, for instance, peat. Since many dikes around the Netherlands are made from a combination of materials further research into other soils could aid in the comprehension of how well-designed the Dutch dikes are considering the effects of drought on soils.
- Interaction with other failure mechanisms: As mentioned dikes may fail due to a variety of mechanisms. Further investigation could delve into the effect of desiccation cracks and their effects on multiple types of failures. This could provide a more comprehensive understanding of dike safety.
- Mitigation: Since this thesis further showed the effect of desiccation cracks on the initiation of piping further research could be undertaken to evaluate possible alternatives for the mitigation of fissures. For example, the use of vegetation as a natural way of protecting flood protection structures.

REFERENCES

Albrecht, B. A., & Benson, C. H. (2001). Effect of Desiccation on Compacted Natural Clays. *Journal of Geotechnical and Geoenvironmental Engineering 127(1)*. https://doi.org/10.1061/(ASCE)1090-0241(2001)127:1(67)

Bernatek-Jakiel, A., & Poesen, J. (2018). Subsurface erosion by soil piping: significance and research needs. *Earth-Science Reviews*, *185*, 1107–1128. https://doi.org/10.1016/j.earscirev.2018.08.006

Bottema, M., Vonk, B., Janssen, H., & van Waveren, H. (2019). *Mitigating drought risk for levees*. 11th ICOLD European Club Symposium.

Foster, M., Fell, R., & Spannagle, M. (2000). A method for assessing the relative likelihood of failure of embankment dams by piping. *Canadian Geotechnical Journal*, *37*(5), 1025–1061. https://doi.org/10.1139/t00-029

Franke, O. L., Reilly, T. E., & Bennett, G. D. (1987). Definition of boundary and initial conditions in the analysis of saturated ground-water flow systems - An introduction. *Techniques of Water-Resources Investigations*. https://doi.org/10.3133/twri03b5

Frontier Economics. (2012). Exploring the links between water and economic growth. In *Circle of Blue*. Corporate Sustainability, HSBC Holdings . https://www.circleofblue.org/wp-content/uploads/2012/06/HSBC_June2012_Exploring-the-links-between-water-and-economic-growth.pdf

Fundamentals of Flood Protection. (2017). Expertise Netwerk Water Veiligheid. https://www.enwinfo.nl/publish/pages/183541/grondslagenen-lowresspread3-v_3.pdf#page22

Gökçekuş, H., & Bolouri, F. (2023). Transboundary Waters and Their Status in Today's Water-Scarce World. *Sustainability*, *15*(5), 4234. https://doi.org/10.3390/su15054234

GRONDSLAGEN VOOR WATERKEREN (p. 79). (1998). TAW. https://www.ecoshape.org/app/uploads/sites/2/2020/10/L7-Grondslagenvoorwaterkeren.pdf

He, J., Wang, Y., Li, Y., & Ruan, X. (2015). Effects of leachate infiltration and desiccation cracks on hydraulic conductivity of compacted clay. *Water Science and Engineering*, *8*(2), 151–157. https://doi.org/10.1016/j.wse.2015.04.004

Illés, Z., & Nagy, L. (2022). Effect of climate change on earthworks of infrastructure: statistical evaluation of the cause of dike pavement cracks. *Geoenvironmental Disasters*, *9*(1). https://doi.org/10.1186/s40677-022-00221-6

Jalil, A., Benamar, A., & Touhami, M. E. (2020). Erosion–Filtration Analysis for Assessing Hydraulic Instability of Dams in Morocco and Global Warming Effect. *Lecture Notes in Civil Engineering*, *90*, 447–454. https://doi.org/10.1007/978-3-030-51354-2_41

Jalil, A., Benamar, A., & Touhami, M. E. (2023). Investigation on the Vulnerability of Core Soils from Three Zoned Dams to Internal Erosion. *Lecture Notes in Civil Engineering*, *370*, 281–295. https://doi.org/10.1007/978-981-99-4041-7_27

Jonkman, S. N. (2014). *An introduction to flood defences*. TU Delft. https://ocw.tudelft.nl/wp-content/uploads/Introduction_to_Water_and_Climate_Reading_material_4_1_2.pdf#page22

Khandelwal, S. (2011). *EFFECT OF DESICCATION CRACKS ON EARTH EMBANKMENTS* (pp. 111–118) [MSc Thesis].

KNMI'23 klimaat scenario's. (2023). KNMI. https://cdn.knmi.nl/system/data_center_publications/files/000/071/901/original/KNMI23_klimaatscenarios_gebruikersrapport_23-03.pdf

Landelijk beeld van de staat van de primaire waterkeringen. (2023). Ministerie van Infrastructuure en Waterstaat.

Musa, J. J., & Gupa, Y. U. (2019). An Overview of Methods Used in the Determination of Soil Hydraulic Conductivity. *Al-Hikmah Journal of Pure & Applied Sciences, 7*.

Omidi, G. H., Thomas, J. C., & Brown, K. W. (1996). Effect of desiccation cracking on the hydraulic conductivity of a compacted clay liner. *Water Air Soil Pollut , 89.* https://doi.org/10.1007/BF00300424

Oñate, E., Díez, P., Zárate, F., & Larese, A. (2008). *Introduction to Finite Element Method*. https://upcommons.upc.edu/bitstream/handle/2117/184007/FEM-Book.pdf

Parker, G. G., & Jenne, E. A. (1967). *Structural Failure of Western Highways Caused By Piping*. Committee on Sub-Surface Drainage. https://onlinepubs.trb.org/Onlinepubs/hrr/1967/203/203-005.pdf#page34

Piet Verschuren, & H Doorewaard. (2010). *Designing a Research Project*. Eleven International Publishing. (Original work published 2007)

Rayhani, M. H., Yanful, E. K., & Fakher, A. (2007). Desiccation-induced cracking and its effect on the hydraulic conductivity of clayey soils from Iran. *Canadian Geotechnical Journal*, *44*(3), 276–283. https://doi.org/10.1139/t06-125

Řehoř, J., Trnka, M., Brázdil, R., Fischer, M., Balek, J., Gerard, & Feng, S. (2023). Global hotspots in soil moisture-based drought trends. *Environmental Research Letters*, *19*(1), 014021–014021. https://doi.org/10.1088/1748-9326/ad0f01

Rivierenland Water Board. (n.d.). *Vastgestelde Legger waterkeringen* [Map]. Rivierenland Water Board. Retrieved April 17, 2024, from https://wsrivierenland.maps.arcgis.com/apps/View/index.html?appid=388180c89db140e9884c57f008e8ff5f

Rivierenland Water Board. (2016). Dwarsprofielen Legger. In *Waterschap Rivierenland*. https://www.waterschaprivierenland.nl/kaarten

Robbins, B. A., & van Beek, V. (2015). *Backward Erosion Piping: A Historical Review and Discussion of Influential Factors*. https://www.researchgate.net/publication/317801148_Backward_Erosion_Piping_A_Historical_Review_and_Discussion_of_Influential_Factors#pf2

Sellmeijer, H., de la Cruz, J. L., van Beek, V. M., & Knoeff, H. (2011). Fine-tuning of the backward erosion piping model through small-scale, medium-scale and IJkdijk experiments. *European Journal of Environmental and Civil Engineering*, *15*(8), 1139–1154. https://doi.org/10.1080/19648189.2011.9714845

Stoop, N. M. (2018). *The effects of anisotropy and heterogeneity in the piping sensitive layer* [MSc Thesis].

Tang, C.-S., Zhu, C., Cheng, Q., Zeng, H., Xu, J.-J., Tian, B.-G., & Shi, B. (2021). Desiccation cracking of soils: A review of investigation approaches, underlying mechanisms, and influencing factors. *Earth-Science Reviews*, *216*, 103586. https://doi.org/10.1016/j.earscirev.2021.103586

Teixeira, A., Wojciechowska, K., & ter Horst, W. (2016). *Derivation of the semi-probabilistic safety assessment for piping*. Deltares.

ter Horst, W. L. A. (2005). *Safety of Dikes during Flood Waves* (pp. 45–46) [MSc Thesis].

Tian, B.-G., Cheng, Q., Tang, C.-S., & Shi, B. (2023). Healing behaviour of desiccation cracks in a clayey soil subjected to different wetting rates. *Engineering Geology*, *313*, 106973–106973. https://doi.org/10.1016/j.enggeo.2022.106973

van Beek, V. (2015). *BACKWARD EROSION PIPING INITIATION AND PROGRESSION* [Thesis].

van Beek, V. (2019). *Use of the 0.3D rule in D-Geo Flow*. Deltares.

van Beek, V., Bezuijen, A., & Sellmeijer, H. (2013). Backward Erosion Piping. *Erosion in Geomechanics Applied to Dams and Levees*, 193–269. https://doi.org/10.1002/9781118577165.ch3

van den Akker, J. J. H., Hendriks, R. F. A., Frissel, J. Y., Oostindie, K., & Wesseling, J. G. (2013). *11th ICOLD European Club Symposium*. Alterra Wageningen UR.

van der Meij, R. (2023). *D-GEO Suite D-Geo Flow Installation manual, tutorial and scientific manual*. Deltares.

van Esch, J. M. (2014). *WTI 2017: Toetsregel Piping* . Deltares. https://www.helpdeskwater.nl/publish/pages/157101/1209435-008-geo-0002-r-final-wti2017-pipingandtransientgroundwaterflow.pdf

van Woudenberg, J. M. (n.d.). *Fragility Curves for Dikes in the Western Scheldt Assessing the Applicability of Typology-Based Fragility Curves in assessing Dike Reinforcement Cost for Coastal Dikes* [MSc Thesis].

VanderSat. (2017). Soil moisture in the Netherlands [Online Image]. In *European Space Agency*. https://www.esa.int/ESA_Multimedia/Images/2017/08/Soil_moisture_in_the_Netherlands

Vergouwe, R., Huting, R. J. M., & van der Scheer, P. (2014). *Overstromingsrisico Dijkring 43 Betuwe, Tieleren Culemborgerwaarden* . Ministerie van Infrastructuur en Milieu, Unie van Waterschappen en Interprovinciaal Overleg.

Wanders, N. (n.d.). Heatwaves and droughts [Interview]. In *Utrecht University*. https://www.uu.nl/en/organisation/in-depth/heatwaves-and-droughts

Ward, P., & Winsemius, H. (n.d.). *River Flood Risk*. Planbureau voor de Leefomgeving. Retrieved April 17, 2024, from https://www.pbl.nl/sites/default/files/downloads/pbl-2018-the-geography-of-future-water-challenges-river-flood-risk_3147.pdf

Weges, H. (2018). Rhine river floods [Online Image]. In *iStock Photo*. https://www.istockphoto.com/es/foto/inunda-r%C3%ADo-rin-gm902621144-248972121

Westerhof, S. G., Booij, M. J., Van den Berg, M. C. J., Huting, R. J. M., & Warmink, J. J. (2022). Uncertainty analysis of risk-based flood safety standards in the Netherlands through a scenario-based approach. *International Journal of River Basin Management*, *21*(3), 559–574. https://doi.org/10.1080/15715124.2022.2060243

APPENDIX

APPENDIX A

This appendix shows the numerical results obtained for Case 1.

Table 13. Results for the scenario with 2 cracks

Run	Minimum H_c with the cracked model (m)	Maximum H_c with the cracked model (m)	Minimum H_c with uncracked model (m)	Maximum H_c with uncracked model (m)	Average difference between cracked and uncracked (m)	Average percentual difference (%)
1	3.44	3.47	4.77	4.82	1.34	27.95
2	3.41	3.43	4.73	4.76	1.33	27.92
3	3.23	3.36	4.53	4.69	1.32	28.53
4	3.37	3.41	4.69	4.74	1.33	28.10
5	3.48	3.5	4.82	4.84	1.34	27.74
6	3.36	3.38	4.68	4.69	1.32	28.07
Average	3.38	3.43	4.70	4.76	1.33	28.05

Table 14. Results for the scenario with 4 cracks

Run	Minimum H_c with the cracked model (m)	Maximum H_c with the cracked model (m)	Minimum H_c with uncracked model (m)	Maximum H_c with uncracked model (m)	Average difference between cracked and uncracked (m)	Average percentual difference (%)
1	3.24	3.38	4.55	4.70	1.32	28.44
2	3.24	3.39	4.55	4.72	1.32	28.48
3	3.42	3.50	4.75	4.85	1.34	27.92
4	3.29	3.36	4.60	4.69	1.32	28.42
5	3.23	3.35	4.53	4.67	1.31	28.48

6	3.23	3.34	4.53	4.67	1.32	28.59
Average	3.28	3.39	4.59	4.72	1.32	28.39

Table 15. Results for the scenario with 6 cracks

Run	Minimum H_c with the cracked model (m)	Maximum H_c with the cracked model (m)	Minimum H_c with uncracked model (m)	Maximum H_c with uncracked model (m)	Average difference between cracked and uncracked (m)	Average percentual difference (%)
1	3.36	3.47	4.68	4.81	1.33	28.03
2	3.25	3.47	4.54	4.81	1.32	28.14
3	3.24	3.50	4.54	4.84	1.32	28.16
4	3.32	3.51	4.64	4.85	1.33	28.04
5	3.24	3.46	4.53	4.80	1.32	28.20
6	3.24	3.40	4.54	4.72	1.31	28.30
Average	3.28	3.47	4.58	4.81	1.32	28.14

Table 16. Results for the scenario with 8 cracks

Run	Minimum H_c with the cracked model (m)	Maximum H_c with the cracked model (m)	Minimum H_c with uncracked model (m)	Maximum H_c with uncracked model (m)	Average difference between cracked and uncracked (m)	Average percentual difference (%)
1	3.30	3.47	4.61	4.81	1.33	28.14
2	3.23	3.49	4.53	4.84	1.33	28.30
3	3.30	3.51	4.61	4.86	1.33	28.10
4	3.30	3.50	4.61	4.85	1.33	28.13
5	3.38	3.49	4.70	4.84	1.34	27.99
6	3.25	3.50	4.55	4.85	1.33	28.20
Average	3.29	3.49	4.60	4.84	1.33	28.14

APPENDIX B

This appendix shows the results of Case 2.

Table 17. Scenario with spacing ranging from 0 to 0.36m

Run	Minimum critical head (m)	Maximum critical head (m)
1	3.24	3.31
2	3.23	3.29
3	3.24	3.27
4	3.33	3.39

5	3.46	3.49
6	3.35	3.39
Average	3.31	3.36

Table 18. Scenario with spacing ranging from 0.36 to 0.60m

Run	Minimum critical head (m)	Maximum critical head (m)
1	3.35	3.43
2	3.31	3.40
3	3.24	3.34
4	3.24	3.33
5	3.35	3.42
6	3.31	3.40
Average	3.30	3.39

Table 19. Scenario with spacing ranging from 0.60 to 1.22m

Run	Minimum critical head (m)	Maximum critical head (m)
1	3.25	3.40
2	3.34	3.47
3	3.28	3.44
4	3.35	3.50
5	3.33	3.47
6	3.34	3.51
Average	3.32	3.47

Table 20. Scenario with spacing ranging from 1.22 to 2.12m

Run	Minimum critical head (m)	Maximum critical head (m)
1	3.25	3.51
2	3.24	3.51
3	3.25	3.5
4	3.23	3.49
5	3.23	3.49
6	3.23	3.50
Average	3.24	3.50

APPENDIX C

This appendix shows the results of Case 3.

Table 21. Scenario with aperture ranging from 0 to 0.008m

Run	Minimum critical head (m)	Maximum critical head (m)
1	3.23	3.39
2	3.37	3.47
3	3.3	3.5
4	3.36	3.46
5	3.40	3.50
6	3.39	3.49
Average	3.34	3.47

Table 22. Scenario with aperture ranging from 0.008 to 0.012m

Run	Minimum critical head (m)	Maximum critical head (m)
1	3.37	3.50
2	3.31	3.44
3	3.36	3.51
4	3.42	3.50
5	3.28	3.40
6	3.28	3.40
Average	3.34	3.46

Table 23. Scenario with aperture ranging from 0.012 to 0.017m

Run	Minimum critical head (m)	Maximum critical head (m)
1	3.30	3.33
2	3.23	3.30
3	3.40	3.50
4	3.43	3.50
5	3.25	3.48
6	3.23	3.39
Average	3.31	3.42

Table 24. Scenario with aperture ranging from 0.017 to 0.025m

Run	Minimum critical head (m)	Maximum critical head (m)
1	3.31	3.49
2	3.31	3.46
3	3.32	3.43
4	3.23	3.44
5	3.24	3.40

6	3.41	3.51
Average	3.30	3.46

APPENDIX D

This appendix displays the link to the repository containing the main models used in the thesis. These include the “Desiccation_cracks_BEP_model” which contains the code for the generation of desiccation cracks and running the critical head calculation, the “Uplift_boundary_BEP_model” in with which critical head calculations can be carried out given specific coordinates for the boundary, and the “Base_model_BEP” which can be run to obtain the base model and calculate critical head values.

https://github.com/ahempel02/Desiccation-cracking-in-D-Geo-Flow

UNIVERSITY OF TWENTE
Drienerlolaan 5
7522 NB Enschede
P.O.Box 217
7500 AE Enschede

P +31 (0)53 489 9111

info@utwente.nl
www.utwente.nl